

REVIEW

Deciphering the Role of Proteoglycans and Glycosaminoglycans in Health and Disease

Alterations in glycosaminoglycan biosynthesis associated with the Ehlers-Danlos syndromes

Delfien Syx,¹ Sarah Delbaere,¹ Catherine Bui,² Adelbert De Clercq,^{1,3} Göran Larson,^{4,5}  Shuji Mizumoto,⁶ Tomoki Kosho,^{7,8} Sylvie Fournel-Gigleux,² and  Fransiska Malfait¹

¹Department of Biomolecular Medicine, Center for Medical Genetics, Ghent University, Ghent, Belgium; ²CNRS IMoPA, Université de Lorraine, Nancy, France; ³Flanders Research Institute for Agriculture, Fisheries and Food (ILVO), Ostend, Belgium; ⁴Department of Laboratory Medicine, Sahlgrenska Academy, University of Gothenburg, Gothenburg, Sweden; ⁵Laboratory of Clinical Chemistry, Sahlgrenska University Hospital, Gothenburg, Sweden; ⁶Department of Pathobiochemistry, Faculty of Pharmacy, Meijo University, Nagoya, Japan; ⁷Center for Medical Genetics, Shinshu University Hospital, Matsumoto, Japan; and ⁸Department of Medical Genetics, Shinshu University School of Medicine, Matsumoto, Japan

Abstract

Proteoglycans consist of a core protein substituted with one or more glycosaminoglycan (GAG) chains and execute versatile functions during many physiological and pathological processes. The biosynthesis of GAG chains is a complex process that depends on the concerted action of a variety of enzymes. Central to the biosynthesis of heparan sulfate (HS) and chondroitin sulfate/dermatan sulfate (CS/DS) GAG chains is the formation of a tetrasaccharide linker region followed by biosynthesis of HS or CS/DS-specific repeating disaccharide units, which then undergo modifications and epimerization. The importance of these biosynthetic enzymes is illustrated by several severe pleiotropic disorders that arise upon their deficiency. The Ehlers-Danlos syndromes (EDS) constitute a special group among these disorders. Although most EDS types are caused by defects in fibrillar types I, III, or V collagen, or their modifying enzymes, a few rare EDS types have recently been linked to defects in GAG biosynthesis. Spondylodysplastic EDS (spEDS) is caused by defective formation of the tetrasaccharide linker region, either due to β 4GalT7 or β 3GalT6 deficiency, whereas musculocontractural EDS (mcEDS) results from deficiency of D4ST1 or DS-epi1, impairing DS formation. This narrative review highlights the consequences of GAG deficiency in these specific EDS types, summarizes the associated phenotypic features and the molecular spectrum of reported pathogenic variants, and defines the current knowledge on the underlying pathophysiological mechanisms based on studies in patient-derived material, in vitro analyses, and animal models.

collagen; decorin; Ehlers-Danlos syndromes; glycosaminoglycan; proteoglycan

INTRODUCTION

Proteoglycans belong to the structurally most complex biomacromolecules in nature and are ubiquitously present in the extracellular matrix (ECM) and on cell surfaces. They consist of a core protein onto which one or more glycosaminoglycan (GAG) chains, such as heparan sulfate (HS), chondroitin sulfate/dermatan sulfate (CS/DS), or keratan sulfate (KS), are covalently attached (1–4). GAGs form long, negatively charged, linear disaccharide repeats and provide proteoglycans with a unique ability to bind water, which is critical for imparting compressive resistance to tissues (3, 5). The backbones of these polysaccharides are made up of two alternating monosaccharides, an amino sugar, either *N*-acetylglucosamine (GlcNAc) or *N*-acetylgalactosamine (GalNAc), and a uronic acid, either glucuronic acid (GlcA) or iduronic acid (IdoA) for

HS and CS/DS, or GlcNAc and galactose (Gal) for KS (5–9). The length of the GAG chains varies, and the sugar residues are modified via epimerization and sulfation reactions, further increasing their structural and functional diversity (10–13). Proteoglycans are critically involved in multiple vital processes during embryonic and postnatal development including cell-cell and cell-matrix interactions, cell proliferation and migration, and cytokine and growth factor signaling. In addition, they are also implicated in several pathological processes such as viral infection, wound repair, tumor growth, and metastasis (2, 14–16). The GAGs also play important roles in the assembly and function of the ECM by interacting with other ECM components, such as collagens, thereby regulating physical properties of the ECM, and by acting as a reservoir for various growth factors (17, 18).

Correspondence: F. Malfait (Fransiska.Malfait@UGent.be).

Submitted 22 March 2022 / Revised 11 August 2022 / Accepted 11 August 2022

<http://www.ajpcell.org>

0363-6143/22 Copyright © 2022 the American Physiological Society.

Downloaded from journals.physiology.org/journal/ajpcell at INSERM (193.054.110.061) on January 25, 2024.



C1843

The biosynthesis of proteoglycan GAG chains is a complex multifaceted process that requires the concerted action of a broad range of enzymes (15, 19–22). Although initiated in the endoplasmic reticulum (ER), it occurs mainly in the Golgi apparatus (23). Assembly of the HS and CS/DS (but not KS) GAG chains is initiated by the biosynthesis of the common tetrasaccharide linker region, which is attached to specific serine residues of the core proteins (GlcA β 1–3Gal β 1–3Gal β 1–4Xyl β 1–O–Ser). This is a stepwise process started by the addition of xylose onto a serine (Ser) residue of the proteoglycan core protein (Fig. 1). The addition of xylose onto a serine residue is catalyzed by xylosyltransferases-I and -II (XylT1 and XylT2), encoded by the paralogs *XYLT1* and *XYLT2* (24, 25). Subsequently, two Gal residues are added by galactosyltransferase-I and -II [β -1,4-galactosyltransferase 7 (β 4GalT7) and β -1,3-galactosyltransferase 6 (β 3GalT6)] encoded by *B4GALT7* and *B3GALT6*, respectively (26, 27). Further addition of a glucuronic acid by glucuronosyltransferase-I [β -1,3-glucuronosyltransferase 3 (β 3GAT3)], encoded by *B3GAT3*, completes the formation of the proteoglycan linker region (28). The linker region can undergo different modifications including sulfation and sialylation of the Gal residues and phosphorylation or fucosylation of the xylose residue (29–31). However, the detailed impact of these modifications on the downstream GAG biosynthesis and the final GAG structure and function is largely unknown. One such modification is the transient phosphorylation of xylose by the kinase FAM20B (32, 33).

Transient phosphorylation of xylose residues is essential for the formation of the linker region, whereas dephosphorylation of xylose residues by 2-phosphoxylose phosphatase 1 (encoded by *PXYLP1*) is required for initiating and efficient elongation of the disaccharide repeat regions of the GAG chains (32). Once the linker region is complete, formation of HS continues with the attachment of a GlcNAc residue by *N*-acetylglucosaminyltransferase-I (exostosin-like glycosyltransferase 2), encoded by *EXTL2*, and the GAG chain is subsequently polymerized by the alternating addition of GlcA and GlcNAc residues by a hetero-oligomeric complex formed by polymerases encoded by *EXT1* and *EXT2* (34–39). Alternatively, formation of CS continues with the attachment of a GalNAc residue by *N*-acetylgalactosaminyltransferase-I (ChGn-1 encoded by *CSGALNACT1*), and the GAG chain is further synthesized by the alternating addition of GlcA and GalNAc residues by bifunctional chondroitin synthases 1–3 (ChSy1–3, encoded by *CHSY1*, *CHSY2*, and *CHSY3*) in association with chondroitin-polymerizing factor (ChPF), encoded by *CHPF* (40–45). The CS moieties are converted to DS moieties by epimerization of the C5 position of GlcA to IdoA, catalyzed by DS epimerase 1 (DS-epi1) or DS epimerase 2 (DS-epi2) encoded by *DSE* or *DSEL*, respectively (46, 47). Immediately after this epimerization reaction, dermatan 4-O-sulfotransferase 1 (D4ST1), encoded by *CHST14*, catalyzes 4-O-sulfation of GalNAc in the IdoA-GalNAc sequence, which prevents backepimerization of IdoA to GlcA (48, 49).

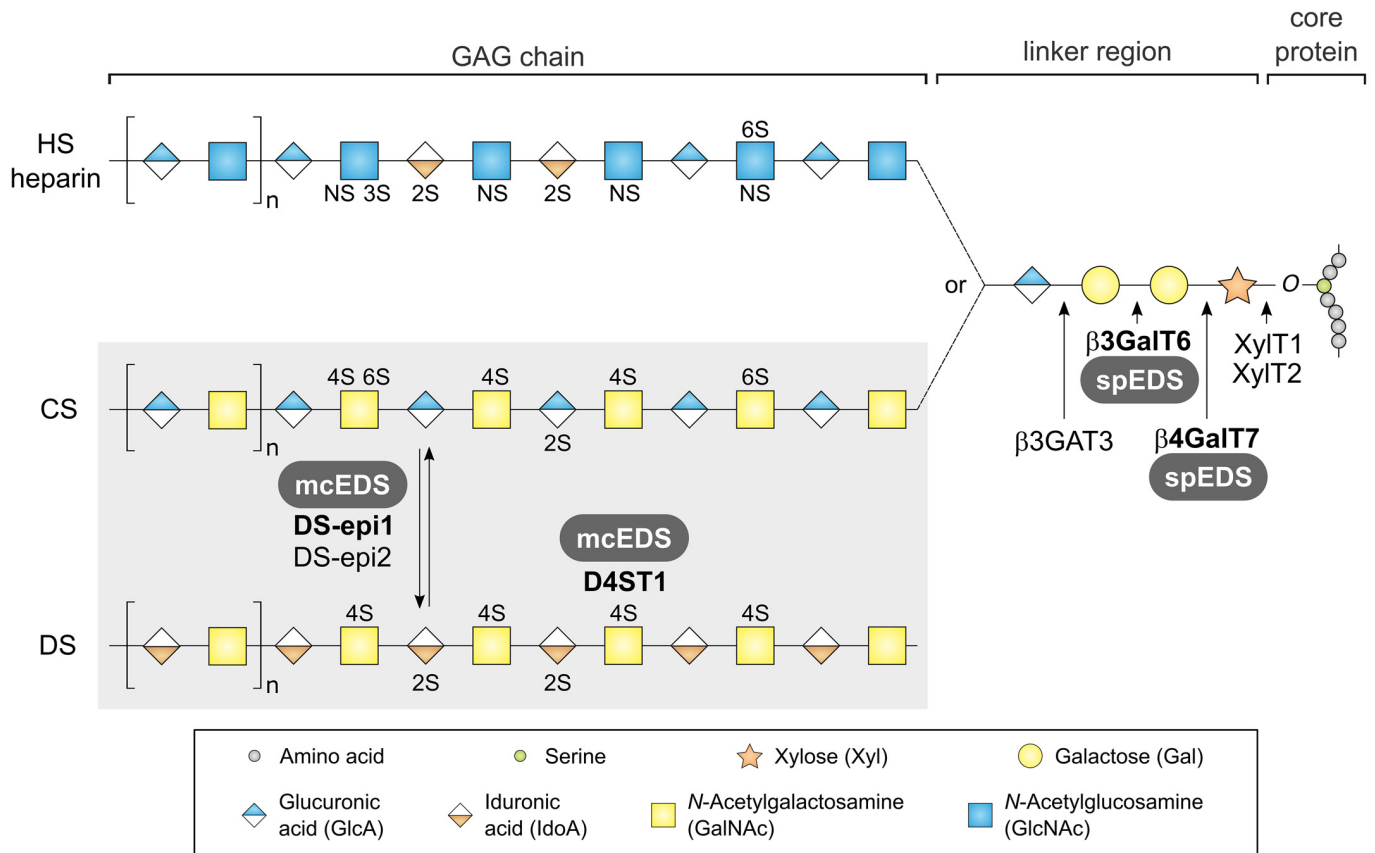


Figure 1. Simplified schematic representation of the proteoglycan linker region and glycosaminoglycan (GAG) biosynthesis. Only a subset of the known GAG modifications is depicted.

Defects in enzymes involved in HS and CS/DS biosynthesis, due to genetic alterations in their respective genes, typically give rise to a range of heritable disorders, including diverse osteochondrodysplasias, multiple exostoses, and specific types of Ehlers-Danlos syndromes (EDS) and have also been associated with cardiac, kidney, and ophthalmological defects, immune deficiencies, and neurological abnormalities (50).

This narrative review will focus specifically on the EDS associated with defects in HS and CS/DS biosynthesis.

THE EHLERS-DANLOS SYNDROMES AND DEFECTS IN GAG BIOSYNTHESIS

The EDS are a clinically and molecularly heterogeneous group of heritable connective tissue diseases. The cardinal features that are common to all EDS types, albeit to different degrees of severity, include joint hypermobility, skin hyperextensibility, and signs of soft connective tissue friability affecting the skin, ligaments, blood vessels, eyes, and internal organs (51). The variability in clinical presentation and severity of the different EDS types is mirrored by the underlying genetic heterogeneity. Based on electron microscopy studies on skin biopsies of affected individuals, EDS was originally suspected to be a collagen disorder (52), and initial biochemical and genetic studies indeed identified defects in the primary structure of the fibrillar types I, III, and V collagen or in their modifying enzymes in individuals with different types of EDS. These discoveries laid the foundation of the 1998 Villefranche EDS Nosology, which was used for over two decades and which included six different EDS types (classical, hypermobility, vascular, kyphoscoliosis, arthrochalasia, and dermatosparaxis) (53). However, advances in molecular techniques expanded the molecular and clinical heterogeneity of this group of syndromes with the identification of defects affecting other ECM molecules, such as ECM-bridging molecules (e.g., tenascin-X, type XII collagen), molecules of the classical complement pathway (C1r and C1s), and, importantly, enzymes involved in GAG biosynthesis (Table 1) (54). As for most of these molecular defects an impact on the collagen fibril architecture was observed, EDS is nowadays considered a “collagen-related disorder,” for which the underlying genetic defects cause alterations in the physical and functional properties of the ECM in essentially all tissues and organs (51).

Upon publication of the 1998 Villefranche classification, the existence of a variant of EDS that was linked to a biochemical defect in GAG biosynthesis, known as “progeroid EDS”, was already recognized, but at the time, this EDS type was not included in the official EDS classification. Hernandez et al. had reported a few individuals presenting signs of EDS in conjunction with a somewhat aged appearance, short stature, and bone deformities (55–57). In 1987, Kresse et al. (58) showed that skin fibroblasts of a child with similar features converted only half of the core protein of decorin, a small leucine-rich proteoglycan (SLRP), to a mature GAG-bearing proteoglycan. This defective GAG biosynthesis was later shown to result from galactosyltransferase-I ($\beta 4\text{GalT7}$) deficiency, and ultimately, biallelic pathogenic variants were identified in the *B4GALT7*

gene (26, 59, 60). This was the first hint toward the implication of defective GAG biosynthesis in the pathophysiology of EDS. Further clues toward a role for defective proteoglycan/GAG biosynthesis in EDS came from the generation of several mouse models in the late nineties. Mice deficient for the core protein of decorin (*Dcn*^{−/−}) showed skin fragility with a marked reduction in tensile strength and abnormal collagen fibril morphology in skin and tendon (61). Signs of connective tissue fragility and ultrastructural collagen fibril abnormalities were also observed in other single and double SLRP-deficient models, summarized in Table 2 (69). As the clinical and ultrastructural observations in these models were highly reminiscent of human EDS, the genes coding for these SLRP core proteins were considered good candidate genes for molecularly unresolved individuals with this disorder. However, no human counterparts were identified upon sequencing of the gene coding for these core proteins (70).

The interest of the EDS research community in defects of GAGs was rekindled a decade later, when several researchers identified, through linkage analysis and homozygosity mapping studies, biallelic pathogenic variants in *CHST14* in several families displaying a phenotype reminiscent of EDS. In 2009, Dündar et al. (71) reported loss-of-function variants in *CHST14* in individuals with adducted thumb-clubfoot syndrome (ATCS), a condition characterized by distal arthrogryposis in conjunction with joint hypermobility, craniofacial features, and other anomalies. In 2010, Kosho et al. reported biallelic mutations in the same gene in a series of Japanese individuals with a phenotype that showed overlap with the kyphoscoliotic type of EDS (the latter caused by deficiency in lysyl hydroxylase 1, a collagen-modifying enzyme), in conjunction with multiple congenital contractures and craniofacial features, and coined it “EDS Kosho type” (72, 73). A follow-up study identified additional biallelic pathogenic variants in the *CHST14* gene (72). The association of *CHST14* with EDS was confirmed by Malfait et al. (74), who also found pathogenic *CHST14* variants in individuals displaying a similar phenotype. These three conditions were grouped together as “musculocontractural EDS” (mcEDS), emphasizing the presence of a musculoskeletal phenotype (“musculo”) and congenital contractures (“contractural”) in combination with EDS(-like) features (74). Not much later, biallelic variants were also found in the *DSE* gene, coding for DS-epil, in a few individuals displaying a mcEDS phenotype (75, 76). A few years later, two groups independently identified biallelic defects in *B3GALT6*, coding for galactosyltransferase-II ($\beta 3\text{GalT6}$) in a series of individuals with an EDS phenotype strongly overlapping with kyphoscoliotic, musculocontractural, and progeroid EDS (77, 78). In view of the strong phenotypic similarities caused by deficiencies of either $\beta 4\text{GalT7}$ or $\beta 3\text{GalT6}$, both conditions are now classified as “spondylodysplastic EDS” (spEDS) to indicate a generalized skeletal dysplasia involving mainly the spine (“spondylo”) in addition to common EDS(-like) characteristics (54).

In the following sections, the phenotypes and mutation spectrum associated with spEDS and mcEDS are discussed. In addition, the pathomechanistic insights gained from in vitro studies and representative animal models for these conditions are summarized.

Table 1. Classification of EDS according to the International EDS Classification, published in 2017 (54)

Nomenclature (abbreviation)	OMIM Number	Gene	Protein	IP	Major Criteria
Defects in collagen primary structure and collagen processing					
Classical EDS (cEDS)	130000	<i>COL5A1</i>	Pro- α 1(V) collagen	AD	Skin hyperextensibility with atrophic scarring
	130010	<i>COL5A2</i>	Pro- α 2(V) collagen		Generalized joint hypermobility
<i>COL1A1</i> -related classical EDS (<i>COL1A1</i> -cEDS)	/	<i>COL1A1</i>	Pro- α 1(I) collagen p. (Arg312Cys)	AD	Skin hyperextensibility with atrophic scarring
					Generalized joint hypermobility
Vascular EDS (vEDS)	130050	<i>COL3A1</i>	Pro- α 1(III) collagen	AD	Arterial rupture at young age
					Spontaneous sigmoid colon perforation in the absence of known colon disease
					Uterine rupture during 3rd trimester of pregnancy
					Carotid-cavernous sinus fistula (in the absence of trauma)
Arthrochalasia EDS (aEDS)	130060	<i>COL1A1</i>	Pro- α 1(I) collagen	AD	Congenital bilateral hip dislocation
	130060	<i>COL1A2</i>	Pro- α 2(I) collagen		Severe generalized joint hypermobility with multiple dislocations
Dermatosparaxis EDS (dEDS)	225410	<i>ADAMTS2</i>	A disintegrin and metalloproteinase with thrombospondin motifs 2 (ADAMTS2)	AR	Skin hyperextensibility
					Extreme skin fragility with congenital or post-natal tears
					Craniofacial features
					Progressively redundant, lax skin with excessive skin folds
					Increased palmar wrinkling
					Severe bruisability
					Umbilical hernia
					Postnatal growth retardation with short limbs
					Perinatal complications related to tissue fragility
Cardiac-valvular EDS (cvEDS)	225320	<i>COL1A2</i>	Pro- α 2(I) collagen	AR	Severe progressive cardiac-valvular insufficiency
					Skin involvement
					Joint hypermobility
Defects in collagen folding and collagen cross-linking					
Kyphoscoliotic EDS (kEDS- <i>PLOD1</i>)	225400	<i>PLOD1</i>	Lysyl hydroxylase 1 (LH1)	AR	Congenital muscle hypotonia
					Congenital or early onset kyphoscoliosis
Kyphoscoliotic EDS (kEDS- <i>FKBP14</i>)	614557	<i>FKBP14</i>	FK506 binding protein 22 kDa (FKBP22)	AR	Generalized joint hypermobility with (sub) luxations
Defects in ECM bridging molecules					
Classical-like EDS (clEDS)	606408	<i>TNXB</i>	Tenascin-X (TNX)	AR	Skin hyperextensibility with velvety skin texture and absence of atrophic scarring
					Generalized joint hypermobility
					Easy bruisable skin/spontaneous ecchymoses
Myopathic EDS (mEDS)	616471	<i>COL12A1</i>	Pro- α 1(XII) collagen	AD/AR	Congenital muscle hypotonia and/or muscle atrophy
					Joint contractures
					Joint hypermobility
Defects in glycosaminoglycan biosynthesis					
Spondylodysplastic EDS (spEDS- <i>B4GALT7</i>)	130070	<i>B4GALT7</i>	Galactosyltransferase-I (β 4GalT7)	AR	Short stature (progressive in childhood)
					Muscle hypotonia (ranging from severe congenital to mild later-onset)
Spondylodysplastic EDS (spEDS- <i>B3GALT6</i>)	615349	<i>B3GALT6</i>	Galactosyltransferase-II (β 3GalT6)	AR	Bowing of limbs
					Skeletal dysplasia
Musculocontractural EDS (mcEDS- <i>CHST14</i>)	601776	<i>CHST14</i>	Dermatan 4-O-sulfotransferase 1 (D4ST1)	AR	Congenital multiple contractures (typically adduction/flexion contractures and talipes equinovarus)
Musculocontractural EDS (mcEDS-DSE)	615539	<i>DSE</i>	Dermatan sulfate epimerase 1 (DS-epi1)	AR	Craniofacial features
					Skin hyperextensibility, easy bruising, skin fragility with atrophic scars
					Increased palmar wrinkling

Continued

Table 1.— Continued

Nomenclature (abbreviation)	OMIM Number	Gene	Protein	IP	Major Criteria
Defects in classical complement pathway					
Periodontal EDS (pEDS)	130080	<i>C1R</i>	Complement C1r (C1r)	AD	Severe and intractable early-onset periodontitis Lack of attached gingiva Pretibial plaques
	617174	<i>C1S</i>	Complement C1s (C1s)		
Defects in intracellular processes					
Spondylodysplastic EDS (spEDS- <i>SLC39A13</i>)	612350	<i>SLC39A13</i>	Zrt/Irt-like Protein 13 (ZIP13)	AR	Short stature (progressive in childhood) Muscle hypotonia (ranging from severe congenital to mild later-onset) Bowing of limbs Skeletal dysplasia Thin cornea with/without rupture
Brittle Cornea Syndrome (BCS)	229200	<i>ZNF469</i>	Zinc finger protein 469 (ZNF469)	AR	
	614170	<i>PRDM5</i>	PR domain-containing protein 5 (PRDM5)		Early-onset progressive keratoconus and/or keratoglobus Blue sclerae
Unresolved forms of EDS					
Hypermobile EDS (hEDS)	130020	?	?	?	Generalized joint hypermobility Systemic manifestations of generalized connective tissue disorder Positive family history Musculoskeletal complaints and pain Exclusion of other EDS types and other joint hypermobility-associated conditions
Novel type of EDS (identified after the 2017 classification)					
Classical-like EDS type 2 (clEDS2) (provisional)	618000	<i>AEBP1</i>	Adipocyte enhancer-binding protein-1 (AEBP1)	AR	Skin hyperextensibility with atrophic scarring Generalized joint hypermobility Foot deformities Early-onset osteopenia

AD, autosomal dominant; AR, autosomal recessive; EDS, Ehlers-Danlos syndrome; IP, inheritance pattern.

THE CLINICAL AND MOLECULAR SPECTRUM OF EDS CAUSED BY DEFECTS IN GAG BIOSYNTHESIS

Spondylodysplastic EDS Due to *B4GALT7* Mutations (spEDS-*B4GALT7*)

To date, homozygous or compound heterozygous (likely) pathogenic variants in *B4GALT7* have been identified in 16 individuals from 11 families (9 males, 6 females, and 1 not reported) displaying a phenotype compatible with spEDS (26, 60, 79–91). Recurring craniofacial features in affected individuals include a short, round face with midface hypoplasia, proptosis, and a narrow mouth. Of note, none of them displayed progeroid features, hence the term “progeroid EDS” was abandoned. Other prominent features include joint hypermobility, especially of the hands, and a soft hyperextensible skin, placing it within the EDS spectrum, and short stature, bowing of the limbs, and radioulnar synostosis. Learning disabilities and ophthalmological abnormalities (especially hypermetropia) were described in about half of the affected individuals. In one family, the phenotype was particularly severe with prenatal or perinatal lethality due to a severe skeletal dysplasia in three consecutive siblings (80). Furthermore, Cartault et al. (86) described a recurring homozygous missense variant in *B4GALT7* [p.(R270C)], in a cohort of 22 patients (11 male, 11 female) with Larsen of Reunion Island syndrome, a skeletal

dysplasia characterized by short stature, joint hypermobility, multiple dislocations, and craniofacial features (Fig. 2A).

The *B4GALT7* gene (NM_007255.3) consists of six coding exons and is located on chromosome 5 (5q35.3). The encoding galactosyltransferase-I protein (β 4GalT7, NP_009186.1) consists of 327 amino acids and contains a short cytoplasmic N-terminal, a transmembrane and a luminal galactosyltransferase domain. In total, 11 missense variants, one nonsense variant resulting in aberrant splicing, one frameshift variant, and one splice site variant with an unknown effect at protein level (p.?) have been identified. The majority of identified variants affects the galactosyltransferase domain (Fig. 3A). The p.(R270C) variant is a recurrent pathogenic variant that has been found in both homozygous and compound heterozygous state, and both in patients diagnosed with EDS or with Larsen of Reunion Island syndrome. The overlap between spEDS-*B4GALT7* and Larsen of Reunion Island syndrome, both in phenotypic and molecular findings, suggests that both conditions belong to the same clinical spectrum (86).

Spondylodysplastic EDS Due to *B3GALT6* Mutations (spEDS-*B3GALT6*)

Biallelic (likely) pathogenic variants in *B3GALT6* have been found in 62 individuals (25 males, 28 females, and 9 not reported) originating from 48 distinct families (77, 78, 81, 90, 92–105). In addition, in one patient, only one mutation was found (78). The clinical diagnoses among these patients ranged

Table 2. Single and double SLRP knock out mouse models

Gene (protein)	Clinical Characteristics	Ultrastructural Collagen Fibril Abnormalities	Reference
Single SLRP knockout mice			
<i>Dcn</i> ^{-/-} (Decorin)	- Skin fragility and laxity - Dermal thinning - Reduced tensile strength	- Variable fibril size and shape - Irregular fibril contours	(61)
<i>Bgn</i> ^{-/-} (Biglycan)	- Dermal thinning - Osteoporosis - Aortic dissection and rupture	- Variable fibril size and shape - Irregular fibril contours	(62, 63)
<i>Lum</i> ^{-/-} (Lumican)	- Skin laxity and fragility - Corneal opacification	- Irregular fibril contours - Increased fibril thickness	(64)
<i>Fmod</i> ^{-/-} (Fibromodulin)	- Reduced tendon stiffness	- Irregular fibril contours - Increase in small diameter fibrils	(65)
Double SLRP knockout mice			
<i>Dcn</i> ^{-/-} / <i>Bgn</i> ^{-/-}	- Severe skin fragility - Marked osteopenia	- Wide interfibrillar spaces - Hieroglyphic appearance	(62)
<i>Lum</i> ^{-/-} / <i>Fmod</i> ^{-/-}	- Gait abnormality - Joint laxity - Age-dependent osteoarthritis	- Irregular fibril contours - Abnormal fibril fusions - Increase in small diameter fibrils	(66, 67)
<i>Bgn</i> ^{-/-} / <i>Fmod</i> ^{-/-}	- Gait impairment - Ectopic tendon ossification - Premature osteoarthritis	- Irregular fibril contours - Increase in small diameter fibrils	(68)

SLRP, small leucine-rich proteoglycan.

from EDS to spondyloepimetaphyseal dysplasia with joint hyperlaxity type 1 (SEMD-JL1) and to Al-Gazali syndrome. Recurring craniofacial features include midfacial hypoplasia with frontal bossing, prominent eyes, and blue sclerae. Other features include joint hypermobility, especially of the hands, a soft hyperextensible skin, kyphoscoliosis (congenital or early onset and progressive), osteopenia with fractures, muscle hypotonia, joint contractures, and radiological features of a spondyloepimetaphyseal dysplasia with metaphyseal widening and bowing of the limb bones, hypoplasia of the iliac bones, acetabular dysplasia, and vertebral body changes. A delay in cognitive development was noted in some affected individuals (81). A few patients suffered from severe vascular problems, including thoracic aortic aneurysms and cerebral hemorrhages (Fig. 2B). Nowadays, it is accepted by clinicians and researchers that biallelic *B3GALT6* defects give rise to a single clinical entity with variable signs of EDS and SEMD-JL1 and the term spEDS-*B3GALT6* is used to describe this pleiotropic disorder (54, 95).

The *B3GALT6* gene (NM_080605.4) is a single exon gene located on chromosome 1 (p36.33) and codes for the galactosyltransferase-II protein (β GalT6, NP_542172.2), a Golgi-resident type II membrane enzyme that consists of 329 amino acids and contains a short amino (N)-terminal cytoplasmic, a transmembrane and a luminal globular catalytic galactosyltransferase domain. So far, 28 missense variants, five in-frame deletions or duplications, seven frameshift variants that give rise to a premature termination codon, one variant affecting the translation initiation codon [p.(M1?)], and one variant disrupting the constitutive stop codon and extending the open reading frame have been reported (Fig. 3B). The identified missense variants are spread over the β GalT6 protein, whereas length-altering variants seem to be located more around the center of the protein. In one patient, the identified variants were not described (105).

Musculocontractural EDS Due to *CHST14* Mutations (mcEDS-*CHST14*)

A total of 70 individuals (34 males, 34 females, and 2 not reported) originating from 50 families have been reported

with homozygous or compound heterozygous (likely) pathogenic variants in *CHST14* (71, 72, 74, 76, 94, 103, 106–117). Recently, Minatogoa et al. (107) collected and reviewed extended clinical and molecular data from 66 of these patients. Recurring craniofacial features include large fontanelle with delayed closure, downslanting and short palpebral fissures, hypertelorism, blue sclerae, small mouth, microretrognathism, and dental abnormalities. Common musculoskeletal features include joint hypermobility with multiple joint dislocations, in combination with multiple congenital contractures, adducted thumbs and progressive talipes deformities, characteristic finger morphologies such as tapering, slender, long, or cylindrical fingers, hypotonia and motor development delay, spinal deformities, and osteoporosis or osteopenia. The skin is often hyperextensible and fragile with atrophic scars, easy bruiseability, palmar wrinkling, and hyperalgesia to pressure. Large subcutaneous hematoma is the most common vascular complication, often occurring at the scalp, buttocks, lower extremities, face, and chest. Other frequently observed complications include constipation, cryptorchidism, and refractive errors. No significant intellectual disability was noted in affected individuals of school age or older (Fig. 2C).

The single exon *CHST14* gene (NM_130468.4) is located on chromosome 15 (15q15.1) and encodes the Golgi-resident D4ST1 protein (NP_569735.1), which consists of 376 amino acids and contains a cytoplasmic domain, a transmembrane domain, and a luminal sulfotransferase domain. A total of 14 missense variants, five nonsense variants, seven frameshift variants introducing a premature termination codon, one frameshift variant creating a longer mutant protein, and one deletion affecting the translation initiation codon [p.(M1?)] have been reported. All identified missense variants are located within or closely adjacent to the catalytic sulfotransferase domain of the D4ST1 protein, in contrast to the variants that introduce a premature termination codon, which are scattered throughout the *CHST14* gene (Fig. 3C).

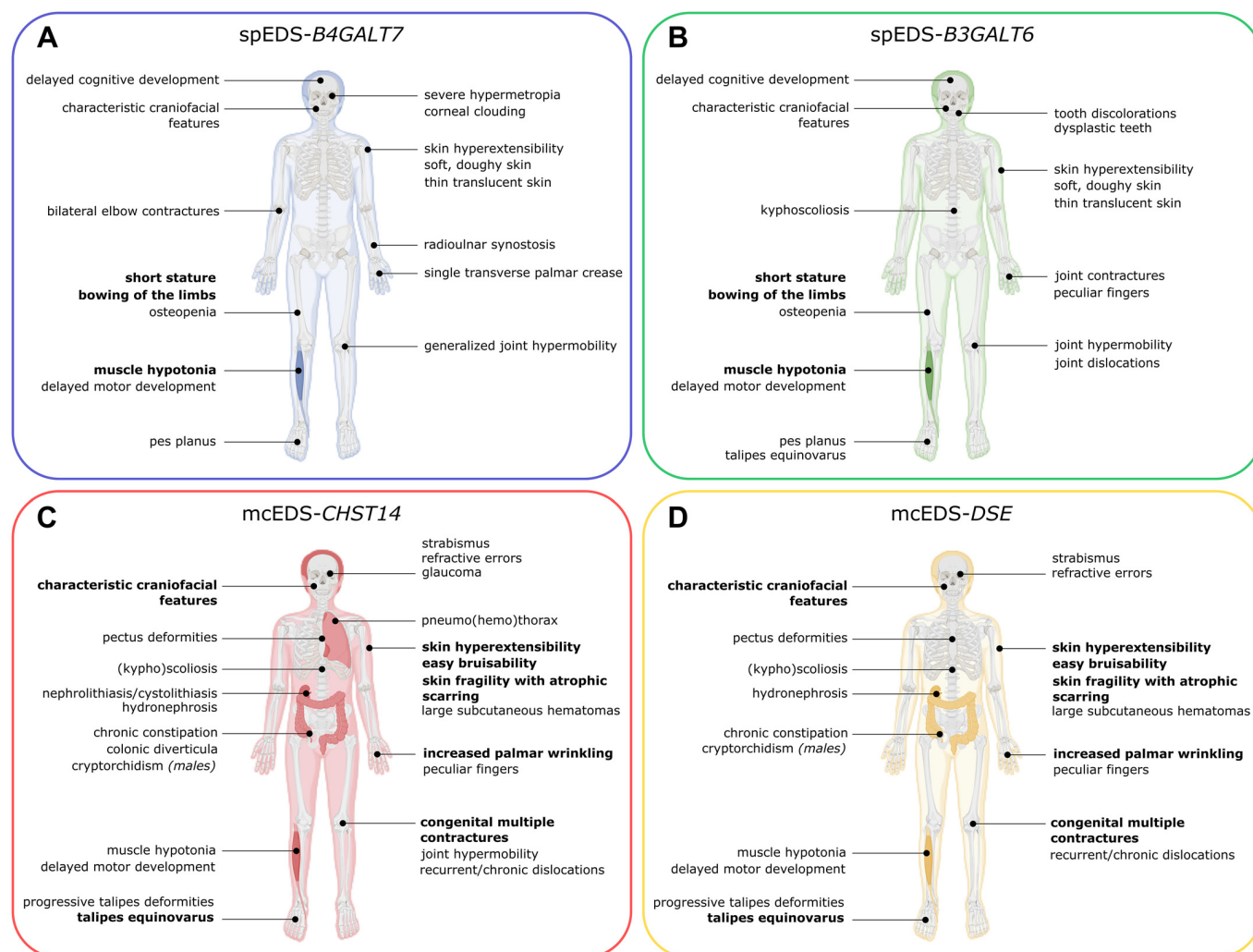


Figure 2. Schematic representation of the clinical features observed in spEDS-*B4GALT7* (A), spEDS-*B3GALT6* (B), mcEDS-*CHST14* (C), and mcEDS-*DSE* (D) based on the major (in bold) and minor diagnostic criteria defined by the 2017 International EDS Classification. Image created with Biorender.com. EDS, Ehlers-Danlos syndrome.

Musculocontractural EDS Due to *DSE* Mutations (mcEDS-*DSE*)

To date, 14 individuals (7 males, 6 females, and 1 not reported) from 8 distinct families have been reported with homozygous (likely) pathogenic variants in *DSE* (75, 76, 90, 118–120). The phenotype associated with mutations in *DSE* is highly similar to that associated with mutations in *CHST14*, but based on the limited number of reported individuals, it appears to be at the milder end of the spectrum. A retrospective study by Minatogawa et al. statistically compared clinical features of 66 patients with mcEDS-*CHST14* with those of 8 patients with mcEDS-*DSE* and found that low-set ears, refractive errors, joint manifestations such as hypermobility with dislocations, skin features, such as hyperextensibility, fragility, bruisability, and atrophic scarring, and constipation were significantly less frequent in patients with mcEDS-*DSE* than with mcEDS-*CHST14* (Fig. 2D) (107).

The *DSE* gene is located on chromosome 6 (6q22.1) and gives rise to different transcripts. The main transcript contains five coding exons (NM_001080976.1), which encodes the 958

amino acid dermatan sulfate epimerase 1 (DS-epi1) protein (NP_001074445.1). The DS-epi1 enzyme is a multispan membrane glycoprotein with an N-terminal epimerase domain residing within the lumen of the Golgi apparatus and two C-terminal transmembrane domains. Currently, eight unique (likely) pathogenic variants in *DSE* have been reported, including four missense variants, one nonsense variant, and three variants introducing a frameshift with a premature termination codon (Fig. 3D) (75, 76, 90, 118–120). All but one of the identified variants affect the epimerase domain, while one missense variant locates to a transmembrane domain.

INSIGHTS INTO THE UNDERLYING PATHOPHYSIOLOGICAL MECHANISMS

Studies addressing the pathophysiological consequences of defects associated with spEDS and mcEDS included biochemical and ultrastructural investigations on patient-derived material, mainly primary dermal fibroblast cultures or skin biopsies, and cellular overexpression assays. In

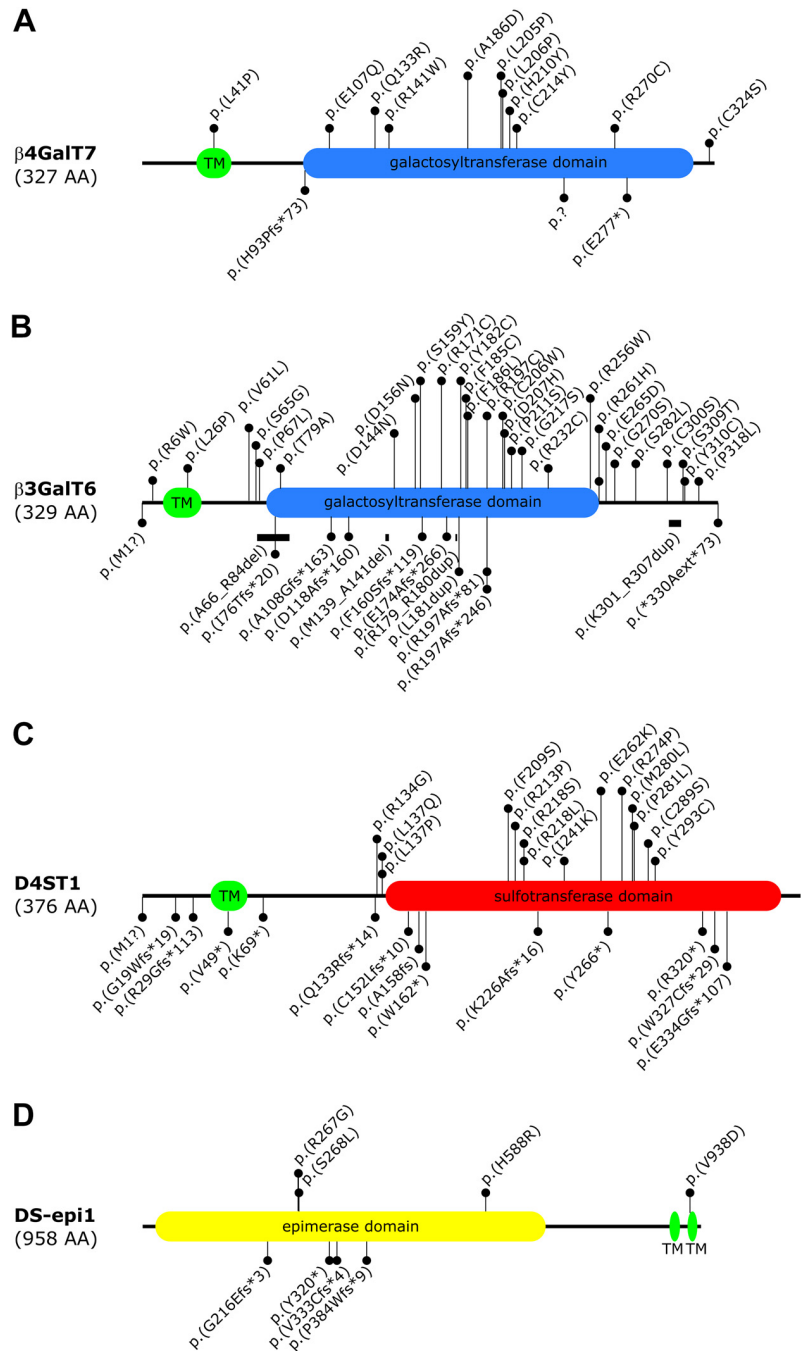


Figure 3. Mutation spectrum associated with spEDS and mcEDS. Schematic representation of $\beta 4$ GalT7 (A), $\beta 3$ GalT6 (B), D4ST1 (C), and DS-epi1 (D). Missense variants are depicted above the protein structure and length-altering variants are depicted below the protein structure. Protein domains were predicted using Pfam in combination with information from literature reports. AA, amino acids; mcEDS, musculocontractural EDS; spEDS, spondylodysplastic EDS; TM, transmembrane domain.

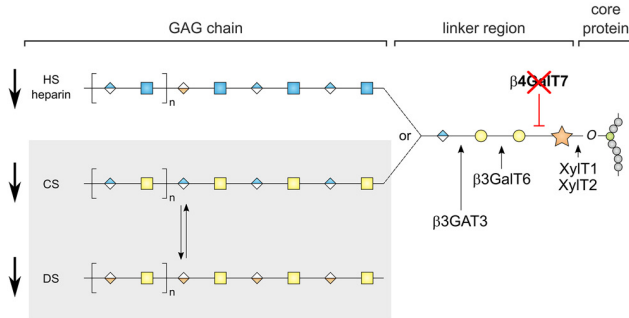
addition, animal models have been of great value for understanding the mechanisms underlying spEDS and mcEDS and to pinpoint tissue-specific alterations. To date, animal models, either mouse or zebrafish, have been generated for all of the GAG biosynthesis defects associated with EDS (121).

spEDS-*B4GALT7*

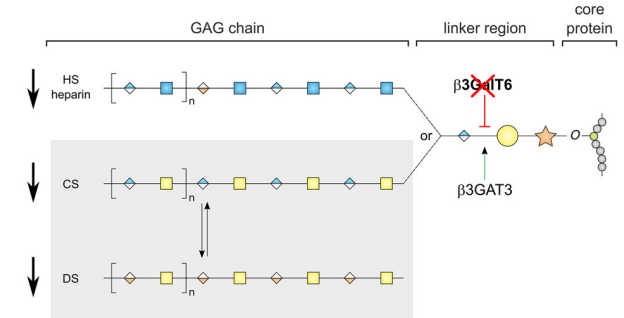
Defects in $\beta 4$ GalT7 affect the biosynthesis of the GAG linker formation by compromising the addition of the second residue, a galactose, to the proteoglycan xylopeptide. Biochemical analyses on dermal fibroblast cultures from patients with spEDS-*B4GALT7* demonstrated reduced in

vitro $\beta 4$ GalT7 activity (59, 122). Consequently, decorin and biglycan core proteins partially substituted by DS GAG chains (58, 122) and reduced epimerization in the decorin GAG chain were observed (122), as well as decreased sulfation of HS chains (123). Western blot analysis for the CS-proteoglycan bikunin demonstrated severely decreased amounts of bikunin-CS and increased levels of GAG-free bikunin core protein in serum from patients with spEDS-*B4GALT7* (Fig. 4A) (124, 125). In addition, overexpression studies for several of the identified missense variants revealed variable, variant-dependent findings, including reduced enzyme activity and/or ability to prime GAG

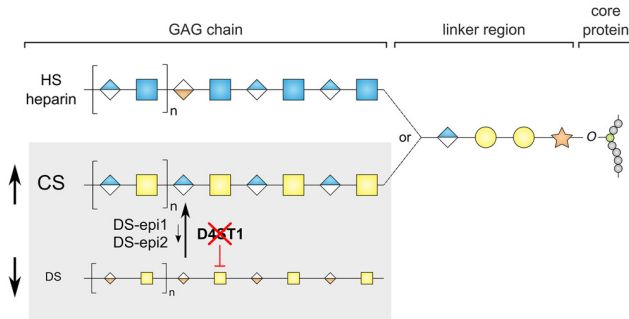
A spEDS-*B4GALT7*



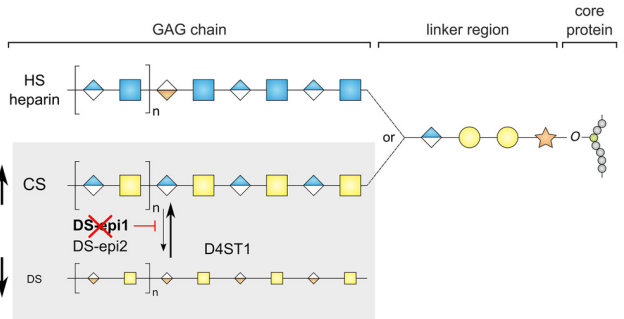
B spEDS-*B3GALT6*



C mcEDS-*CHST14*



D mcEDS-*DSE*



E

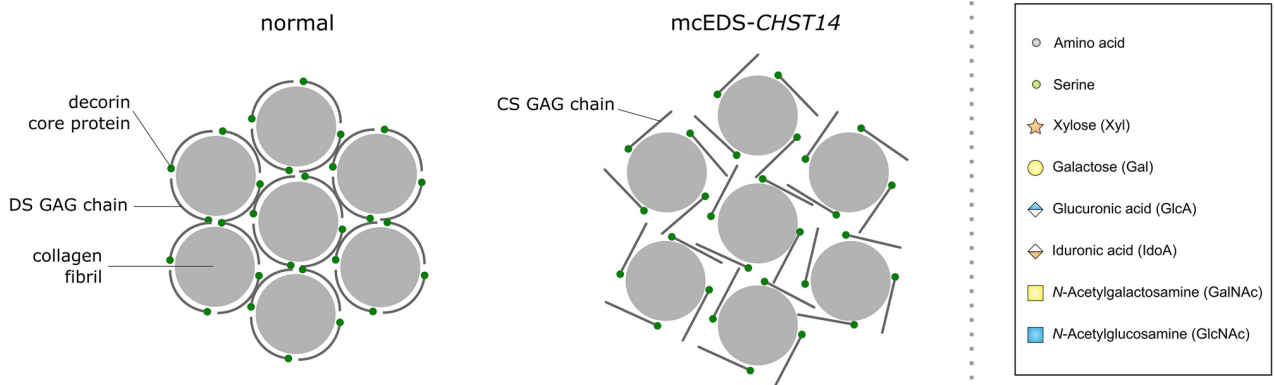


Figure 4. Currently known pathomechanisms associated with spEDS and mcEDS. **A:** $\beta 4\text{GalT7}$ deficiency in patients with spEDS-*B4GALT7* results in severely reduced levels of HS, CS, and DS chains. **B:** in patients with spEDS-*B3GALT6*, an unconventional trisaccharide linker region is formed. $\beta 3\text{GalT6}$ deficiency results in severely reduced levels of HS, CS, and DS chains. **C:** D4ST1 deficiency in mcEDS-*CHST14* prevents sulfation of GalNAc residues, as such IdoA is backepimerized to GlcA by DS-epi1/2, which results in absence of DS while increased CS levels are identified. **D:** deficiency of DS-epi1 in mcEDS-*DSE* results in decreased epimerization of GlcA to IdoA, hence only limited GalNAc residues can be sulfated by D4ST1 and limited DS moieties are formed. Consequently, higher amounts of CS are detected. **E:** replacing the flexible DS chain of decorin (normal) by the rigid CS chain in patients with mcEDS-*CHST14* can contribute to the spatial disorganization of collagen fibrils in patients with mcEDS-*CHST14*. Sulfated residues are not indicated in this figure. CS, chondroitin sulfate; DS, dermatan sulfate; HS, heparan sulfate; mcEDS, musculocontractural EDS; spEDS, spondylodysplastic EDS.

biosynthesis (80, 126), diminished mutant $\beta 4\text{GalT7}$ protein levels (80, 127), or intracellular mislocalization of mutant $\beta 4\text{GalT7}$ proteins (60, 80). Furthermore, spEDS-*B4GALT7* fibroblasts were reported to show morphological alterations with intracellular accumulation of lysosomes and vacuoles, decreased proliferation rate, and delayed in vitro wound closure (122, 123). Fibroblasts from patients with spEDS-*B4GALT7* produced a disorganized ECM and perturbed deposition of type I collagen (122, 123).

To further study the pathogenic mechanisms underlying spEDS-*B4GALT7*, Delbaere et al. (128) generated homozygous *b4galt7* knockout (*b4galt7*^{-/-}) zebrafish. At 4 days postfertilization (dpf), *b4galt7*^{-/-} zebrafish totally lacked HS and CS GAGs, resulting in a severe skeletal phenotype with delayed or absent ossification of several bone structures and aberrant cartilage formation. These zebrafish died before the age of 10 dpf, suggesting that complete loss of $\beta 4\text{GalT7}$ activity is incompatible with life in zebrafish. As complete loss of $\beta 4\text{GalT7}$

function is not seen in human patients with spEDS-*B4GALT7*, hypomorphic zebrafish were generated, which display only partial loss of β 4GalT7 function and better mimic the variable decrease in β 4GalT7 activity seen in patients with spEDS-*B4GALT7*. Two distinct morpholino-based *b4galt7* knock-down (morphant) and two mosaic *b4galt7*-deficient (crispant) models were created (128). In these models, defective β 4GalT7 activity led to hampered GAG biosynthesis with severely diminished HS and CS proteoglycan levels. Compared to the craniofacial abnormalities and short stature seen in patients with spEDS-*B4GALT7*, morphant and crispant *b4galt7* embryos showed underdeveloped, misshapen, and partly absent cartilage structures during early development and were smaller than wild-type (WT) embryos. In addition, severely reduced or absent ossified bone structures reminiscent of osteopenia were seen in some patients with spEDS-*B4GALT7*. Compromised muscle function and structure were seen in one *b4galt7* morphant model, which is in line with the muscle hypotonia and delayed motor development present in patients with spEDS-*B4GALT7*. Taken together, these results indicate that juvenile *b4galt7* zebrafish models largely phenocopy the human spEDS-*B4GALT7* phenotype (128).

Interestingly, spontaneous *B4GALT7* defects have also been identified as a cause of disproportionate dwarfism with joint laxity in Frisian horses (129).

These findings highlight a key role for β 4GalT7 in early development and in cartilage, bone, and possibly muscle formation and illustrate that defective β 4GalT7 alters the biosynthesis of both CS/DS and HS, which underlies the spEDS-*B4GALT7* phenotype. Moreover, the type and location of the variant, its effect on protein structure, and the influence on enzyme activity and/or intracellular localization of the mutant enzyme result in variant-specific outcomes that can account for the variability in phenotypic severity seen in patients with spEDS-*B4GALT7*.

spEDS-*B3GALT6*

The β 3GalT6 enzyme catalyzes the addition of the third monosaccharide residue, a Gal, to the linker region. Studies on dermal fibroblast cultures from patients with biallelic *B3GALT6* defects indicated that at least some of the identified variants give rise to reduced β 3GalT6 protein levels (95). In addition, overexpression studies illustrated intracellular mislocalization of some mutant β 3GalT6 proteins in contrast to the typical localization to the Golgi localization observed in control fibroblasts (78, 93). spEDS-*B3GALT6* fibroblasts display severely reduced galactosyltransferase activity using specific synthetic compounds but are still able to prime GAG biosynthesis when incubated with an exogenous substrate such as 4-MUX (77, 78, 95). As a consequence, GAG biosynthesis was strongly diminished in patient fibroblasts with severely impaired glycosylation of the decorin core protein (77, 93, 95) as well as decreased HS production (Fig. 4B) (77, 95, 102). Notably, disaccharide analysis of GAGs produced by patient-derived lymphoblastoid cells showed decreased HS, but an increase for CS and DS disaccharides (78). Similar to patients with spEDS-*B4GALT7*, Western blot analysis also indicated the presence of GAG-free bikunin in serum of patients with spEDS-*B3GALT6* (124, 125). Transmission electron microscopic analysis on skin biopsies of patients with spEDS-*B3GALT6*

showed dispersed and loosely packed collagen fibrils in the dermis, with variable collagen fibril diameters and occasional fibrils with very irregular contours (77, 95). In vitro deposition of type III and type V collagen and recruitment of the collagen-specific α 2 β 1 integrin by dermal fibroblasts was also disturbed in patients with spEDS-*B3GALT6* (102). In addition, delayed in vitro wound closure was observed (77, 95). Microarray-based transcriptome profiling performed on dermal fibroblast cultures from two affected sisters illustrated deregulated expression of genes coding for ECM molecules, enzymes responsible for ECM remodeling and GAG biosynthesis, and TGF β /BMP signaling pathway (102).

To gain more insights into the underlying pathomechanisms of spEDS-*B3GALT6*, homozygous *b3galt6* knockout (*b3galt6*^{-/-}) zebrafish were generated. These *b3galt6*^{-/-} zebrafish survived to adulthood, contrasting the early lethal phenotype of *b4galt7*^{-/-} zebrafish (130). Furthermore, *b3galt6*^{-/-} zebrafish showed progressive skeletal malformations with variable severity, reminiscent of the variable skeletal dysplasia phenotype observed in patients with spEDS-*B3GALT6*. Ultrastructural analysis in adult *b3galt6*^{-/-} zebrafish showed less organized type I collagen fibers in the intervertebral ligament (the outer type I collagen layers) and the inner layer of the vertebral bone that is first deposited during development, and a thicker epidermis covering the scales with loosely packed dermal collagen fibrils with increased interfibrillar spaces. The latter findings mimic ultrastructural features of patients with spEDS-*B3GALT6* and could be attributed to alterations in the GAG chains of SLRPs, which regulate collagen fibrillogenesis. In addition, structural and functional muscle abnormalities were detected in *b3galt6*^{-/-} zebrafish, consistent with the muscle hypotonia and delayed motor development observed in human patients. The phenotypic findings are in accordance with the strongly reduced amounts of CS, DS, and HS-disaccharides observed in bone, skin, and muscle of *b3galt6*^{-/-} zebrafish. Surprisingly, low amounts of GAGs were still produced by *b3galt6*^{-/-} zebrafish, and residual proteoglycans were shown to contain a noncanonical trimeric linker region consisting of only three instead of four sugars (lacking a galactose residue), thereby presenting a possible rescue mechanism for deficiency of one of the linker enzymes. The presence of this noncanonical trimeric linker region was originally found in very low amounts in urine of healthy individuals (131) but a drastically increased level was recently detected in urine samples of human patients with spEDS-*B3GALT6* (132). Overall, *b3galt6*^{-/-} zebrafish phenocopy human spEDS-*B3GALT6* and present craniofacial dysmorphism, generalized skeletal dysplasia, skin involvement, and indications of muscle hypotonia.

Taken together, the findings in patients with spEDS-*B3GALT6* and *b3galt6*^{-/-} zebrafish emphasize the importance of proper GAG biosynthesis for collagen fibrillogenesis, general ECM assembly, and several physiological functions necessitating proper connective tissue function, such as wound healing.

mcEDS-*CHST14*

Genetic alterations in mcEDS-*CHST14* compromise the function of D4ST1, an enzyme that is specifically involved in the biosynthesis of DS, by catalyzing 4-O-sulfation of GalNAc

in the IdoA-GalNAc sequence. Defects in D4ST1 result in significantly lower sulfotransferase activity in dermal fibroblast cultures from patients with mcEDS-*CHST14* and in cell models overexpressing mutant D4ST1 (72). Analysis of the disaccharide composition of CS/DS chains isolated from fibroblasts of patients with mcEDS-*CHST14* showed negligible amounts of DS and an excessive presence of CS (71, 72). In addition, urinary disaccharide analysis also showed absence of DS, indicating a systemic depletion of DS in patients with mcEDS-*CHST14* (133). 4-O-sulfation in CS and DS is known to inhibit the function of DS-epi1 and DS-epi2 (134). Hence, D4ST1 deficiency impairs 4-O-sulfation and thus allows back-epimerization of IdoA to GlcA, thereby favoring the formation of CS (Fig. 4C). Decorin, a major DS-proteoglycan in skin, plays an important role during collagen fibril formation, possibly through electrostatic interactions between its GAG chains and adjacent collagen fibrils (135). The single GAG chain of decorin was shown to be substituted by CS and excessive CS GAGs were detected in patient fibroblasts (72, 76, 106, 116). Transmission electron microscopy on skin biopsies from patients with mcEDS-*CHST14* showed dermal collagen fibrils that were dispersed and less tightly packed throughout the dermis with increased interfibrillar space (72, 76, 106, 110). In addition, electron microscopy-based visualization of GAG chains in skin demonstrated the presence of linear GAG chains that projected from the outer surface of the collagen fibrils, in contrast to curved GAG chains that maintain close contact with collagen fibrils in healthy control samples (Fig. 4E) (136). As such, replacing the flexible DS chain of decorin by the rigid CS chain can contribute to the spatial disorganization of collagen fibrils in patients with mcEDS-*CHST14*. Furthermore, in vitro deposition was disturbed for several ECM components, including types I, III, and V collagen, by mcEDS-*CHST14* fibroblasts (76, 106, 116).

Although diverse studies on different homozygous *Chst14* knockout (*Chst14*^{-/-}) mouse models have been performed, investigations on *Chst14*^{-/-} mice are hampered by the high perinatal lethality of the animals (137). Perinatal lethality is rarely observed in patients with mcEDS-*CHST14* but is often encountered in rodent models and could be attributed to genetic background or placental factors. Placental dysplasia was indeed demonstrated in *Chst14*^{-/-} mice, with reduced weight of the placenta, alteration in the vascular structure with ischemic and/or necrotic-like change, an abnormal structure of the basement membrane of capillaries in the placental villus, and significantly decreased DS (137). These findings suggest that DS may be essential for placental vascular development. Mice deficient for *Chst14* showed growth impairment with smaller body mass, reduced fertility, kinked tail, and increased skin fragility (138, 139). Moreover, the skin of *Chst14*^{-/-} mice showed decreased amounts of DS and elevated CS levels. Similar to the findings in patients with mcEDS-*CHST14*, rod-shaped linear GAG chains that protruded outside of the collagen fibrils were found in *Chst14*^{-/-} mice, in contrast to those being round and wrapping around the collagen fibrils in wild-type mice (139, 140). Furthermore, *Chst14*^{-/-} mice showed thoracic kyphosis and myopathy-related phenotypes such as lower grip strength and decreased exercise capacity, with decreased DS in muscle and variation in fiber size and spread of the muscle interstitium (139, 141). In addition, *Chst14*^{-/-} mice provided

evidence for an overall negative impact of DS on peripheral nerve regeneration (138) but beneficial activity in central nervous system regeneration, which could result from differences in DS proteoglycans levels and their interaction partners between the peripheral and central nervous systems (142). *Chst14*^{-/-} mice also showed impaired spatial learning and memory and demonstrated that DS is indispensable for synaptic plasticity in the hippocampus, which might be attributed to impaired Akt/mTOR-signaling (143).

Together, the findings in patients with mcEDS-*CHST14* and *Chst14*^{-/-} mice point to a role for DS in versatile functions and in different tissues, including skin, muscle, nervous system, and highlight its importance for proper spacing of collagen fibrils and ECM integrity.

mcEDS-DSE

Epimerization of GlcA to IdoA, catalyzed by DS-epi1 or DS-epi2, is required for sulfation of an adjacent GalNAc residue by D4ST1 which is necessary to form DS. DS-epi1 appears to be the predominant epimerase in most tissues and can produce long stretches of IdoA containing disaccharide units, whereas DS-epi2 mainly functions in the brain and forms only short IdoA blocks (10). Biallelic pathogenic variants in *DSE* severely compromise DS-epi1 activity both in patient fibroblasts and of recombinant mutant DS-epi1 enzyme (75). A markedly reduced amount of DS disaccharides and an increased amount of CS disaccharides were demonstrated in fibroblasts from a patient with mcEDS-DSE, consistent with increased synthesis or reduced conversion of CS chains (75). In addition, a minor fraction of DS was detected in the GAG chain of decorin produced by patient fibroblasts (75, 76). In contrast to the complete loss of DS in mcEDS-*CHST14*, the preservation of DS moieties in fibroblasts from patients with mcEDS-DSE is indicative of residual activity of mutant DS-epi1 or partial compensation by DS-epi2 (Fig. 4D). Although CS cannot generally substitute for DS-specific functions, the residual availability of some DS disaccharide units might contribute to the attenuated phenotype in mcEDS-DSE. The measurement of the disaccharide compositions of DS and CS chains in a urine sample demonstrated the lack of DS in the urine sample, suggesting that this test may also be a useful screening method for mcEDS-DSE (118).

Before genetic defects in *DSE* were identified in patients with mcEDS, homozygous *Dse* knockout (*Dse*^{-/-}) mice were already generated (144). *Dse*^{-/-} mice were smaller, presented with a kinked tail that resolved before 4 wk of age and had reduced fertility. The skin of *Dse*^{-/-} mice had reduced tensile strength and sparser loose hypodermal connective tissue despite normal collagen content. TEM analysis revealed dermal collagen fibrils with larger diameters but normal fibril density, whereas *Dse*^{-/-} tail tendons showed only a minor shift toward thicker fibrils with mostly fibrils with normal diameter and no differences in diameter in Achilles tendon (144). This contrasts the normal ultrastructure of dermal collagen fibrils in patients with mcEDS-DSE, although morphometric analysis was not performed (76). Furthermore, impairment of directional migration of aortic smooth muscle cells and defects in the fetal abdominal wall, exencephaly, and spina bifida were seen in *Dse*^{-/-} mice (144, 145). DS-epi2-deficient mice (*Dse1*^{-/-}) had no anatomical, histological, or morphological abnormalities despite reduced epimerase activity (10). As

such, DS-epi1 might compensate for the function of DS-epi2. Double knockout mice of *Dse* and *Dsel* exhibited perinatal lethality with umbilical hernia, exencephaly, a kinked tail, and complete loss of DS, suggesting that DS plays an important role in embryonic development and perinatal survival (146).

Although patients with mcEDS-DSE presumably show a milder phenotype, the limited number of patients precludes firm statements. Nevertheless, findings in both patients and mouse models indicate the importance of DS-epi1 function, which cannot be fully substituted by DS-epi2.

CONCLUSIONS AND PERSPECTIVES

To date, the role of abnormal GAG biosynthesis in EDS pathogenesis has been firmly established by the identification of defects in four biosynthetic enzymes, which are either involved in the biosynthesis of the tetrasaccharide linker region or the modification of GAG chains. Whereas defective linker formation in spEDS, due to deficiency of either β 4GalT7 or β 3GalT6, affects the biosynthesis of both HS and CS/DS GAG chains, the defects in D4ST1 and DS-epi1 associated with mcEDS, specifically compromise DS biosynthesis. The key role of proper GAG biosynthesis and the crucial biological functions of proteoglycans are reflected in the pleiotropic phenotypes of both spEDS and mcEDS, with the perturbation of many physiological functions that are critical for the correct architecture and homeostasis of various connective tissues. The identification of additional patients and follow-up of identified patients will likely expand the phenotypic spectrum and will allow to determine the natural history of these rare EDS types.

Molecular diagnosis of both spEDS and mcEDS relies on the identification of a genetic defect in the corresponding disease genes. Targeted gene panel analysis or whole exome sequencing are the molecular methods of choice when spEDS or mcEDS is suspected, given the phenotypic overlap between the conditions as well as with other EDS types or other disorders, such as skeletal dysplasia. Interestingly, specific urine and serum analyses might provide a reliable method for diagnosing spEDS and mcEDS, although these analyses are not (yet) routinely implemented in a diagnostic setting. Urinary disaccharide compositional analysis of CS/DS chains provides a noninvasive screening method for mcEDS (118, 133). In addition, the detection of increased amounts of GAG-free bikunin core protein in serum by Western blot analysis could function as a biomarker for spEDS (124, 125, 147).

Important gaps remain in our understanding of how these GAG defects give rise to the corresponding phenotype. It is still unclear to what extent different aspects of GAG chain biosynthesis are affected in spEDS and mcEDS, including 1) the length and modification of GAG chains, 2) modification and composition of the linker region, 3) if preferential production of certain proteoglycans occurs when GAG biosynthesis is restricted, and 4) whether these alterations occur in a tissue-specific manner. Furthermore, the consequences on other interacting molecules, such as, for example, collagens and other ECM components and how these changes affect physiological processes, such as wound healing, bone formation etc., need more investigation.

Especially for these rare EDS types, the use of animal models can be of great help to start addressing these gaps and allow spatiotemporal investigations. *Chst14*^{-/-} and *Dse*^{-/-} murine models have been shown to phenocopy aspects of their human mcEDS counterparts. Studies on *b4galt7* and *b3galt6* zebrafish models provided proof-of-concept that zebrafish are a powerful tool to study the phenotypic and bio-molecular consequences of impaired GAG linker region synthesis and further underscore their usefulness as animal models for EDS research, as illustrated by the identification of an unconventional trilinear region in *b3galt6*^{-/-} zebrafish. The presence of this potential rescue mechanism in zebrafish and patients with spEDS-B3GALT6 could possibly explain why these animals and patients can survive. In contrast, *b4galt7*^{-/-} zebrafish do not survive past 10 dpf and increased early lethality can possibly explain why less patients with B4GALT7 variants have been reported. Nevertheless, in depth analyses of the linker region in *b4galt7*^{-/-} zebrafish and patients with spEDS-B4GALT7 is yet to be done. Moreover, the generation of stable knock-in models harboring (reported) missense variants could overcome the reported phenotypic variability of *b4galt7* crispants and lethality of the *b4galt7*^{-/-} knockout zebrafish and would allow to study the adult phenotype in more depth (128). In addition, a combination of transcriptomic and proteomic approaches, both in animal models and human samples, could unravel spatiotemporal changes and consequences. As such, the identification of distinct and/or common pathways that are affected in spEDS and mcEDS could provide an explanation, at least in part, for the phenotypic differences and overlap seen between these conditions.

The current treatment and management options for patients with EDS are limited and no targeted therapy is available for spEDS or mcEDS. Therefore, the elucidation of the underlying pathogenic mechanisms and deregulated pathways will likely expose novel druggable targets. The introduction of zebrafish into the EDS research field therefore also holds promising potential for therapeutic discovery, given the highly amenability of this model for drug/compound screening.

ACKNOWLEDGMENTS

This article is part of the special collection “Deciphering the Role of Proteoglycans and Glycosaminoglycans in Health and Disease.” Dr. Liliana Schaefer served as Guest Editor of this collection.

GRANTS

This work is supported by the Research Foundation Flanders (12Q5920N to D.S., 1842323N and G0A3322N to F.M.), the Ehlers-Danlos Society, Ghent University (GOA019-21), the Swedish state under the agreement between the Swedish Government and the county councils, the ALF agreement (ALFGBG_721971 to G.L.), in part by a Grant-in Aid for Scientific Research from the Japan Society for the Promotion of Science, Japan (19K07054 to S.M.), the Union Nationale de Syndromes d'Ehlers-Danlos (UNSED) patient's association (to S.F.-G.), the ESPOIR caritative association (to S.F.-G.), and Université de Lorraine Action Incitative fund (to C.B.).

DISCLOSURES

No conflicts of interest, financial or otherwise, are declared by the authors.

AUTHOR CONTRIBUTIONS

D.S. prepared figures; D.S. and F.M. drafted manuscript; D.S., S.D., C.B., A.D.C., G.L., S.M., T.K., S.F-G., and F.M. edited and revised manuscript; D.S., S.D., C.B., A.D.C., G.L., S.M., T.K., S.F-G., and F.M. approved final version of manuscript.

REFERENCES

- Bishop JR, Schuksz M, Esko JD. Heparan sulphate proteoglycans fine-tune mammalian physiology. *Nature* 446: 1030–1037, 2007. doi:10.1038/nature05817.
- Couchman JR, Pataki CA. An introduction to proteoglycans and their localization. *J Histochem Cytochem* 60: 885–897, 2012. doi:10.1369/0022155412464638.
- Prydz K, Dalen TK. Synthesis and sorting of proteoglycans. *J Cell Sci* 113: 193–205, 2000. doi:10.1242/jcs.113.2.193.
- Höök M, Kjellén L, Johansson S. Cell-surface glycosaminoglycans. *Annu Rev Biochem* 53: 847–869, 1984. doi:10.1146/annurev.bi.53.070184.004215.
- Rodén L. Structure and metabolism of connective tissue proteoglycans. In: *The Biochemistry of Glycoproteins and Proteoglycans*, edited by Lennarz WJ. New York: Springer, 1980, 267–371.
- Pomin V, Mulloy B. Glycosaminoglycans and proteoglycans. *Pharmaceuticals (Basel)* 11: 27, 2018. doi:10.3390/ph11010027.
- Kjellén L, Lindahl U. Proteoglycans: structures and interactions. *Annu Rev Biochem* 60: 443–475, 1991 [Erratum in *Annu Rev Biochem* 61: following viii, 1992]. doi:10.1146/annurev.bi.60.070191.002303.
- Funderburgh JL. Keratan sulfate: structure, biosynthesis, and function. *Glycobiology* 10: 951–958, 2000. doi:10.1093/glycob/10.10.951.
- Sugahara K, Mikami T, Uyama T, Mizuguchi S, Nomura K, Kitagawa H. Recent advances in the structural biology of chondroitin sulfate and dermatan sulfate. *Curr Opin Struct Biol* 13: 612–620, 2003. doi:10.1016/j.sbi.2003.09.011.
- Thelin MA, Bartolini B, Axelsson J, Gustafsson R, Tykesson E, Pera E, Oldberg Å, Maccarana M, Malmstrom A. Biological functions of iduronic acid in chondroitin/dermatan sulfate. *FEBS J* 280: 2431–2446, 2013. doi:10.1111/febs.12214.
- Kusche-Gullberg M, Kjellén L. Sulfotransferases in glycosaminoglycan biosynthesis. *Curr Opin Struct Biol* 13: 605–611, 2003. doi:10.1016/j.sbi.2003.08.002.
- Xu D, Esko JD. Demystifying heparan sulfate-protein interactions. *Annu Rev Biochem* 83: 129–157, 2014. doi:10.1146/annurev-biochem-060713-035314.
- Mizumoto S, Yamada S, Sugahara K. Molecular interactions between chondroitin-dermatan sulfate and growth factors/receptors/matrix proteins. *Curr Opin Struct Biol* 34: 35–42, 2015. doi:10.1016/j.sbi.2015.06.004.
- Kaur SP, Cummings BS. Role of glypicans in regulation of the tumor microenvironment and cancer progression. *Biochem Pharmacol* 168: 108–118, 2019. doi:10.1016/j.bcp.2019.06.020.
- Mikami T, Kitagawa H. Biosynthesis and function of chondroitin sulfate. *Biochim Biophys Acta* 1830: 4719–4733, 2013. doi:10.1016/j.bbagen.2013.06.006.
- Diehl V, Huber LS, Trebicka J, Wygrecka M, Iozzo RV, Schaefer L. The role of decorin and biglycan signaling in tumorigenesis. *Front Oncol* 11: 801801, 2021. doi:10.3389/fonc.2021.801801.
- Schaefer L, Schaefer RM. Proteoglycans: from structural compounds to signaling molecules. *Cell Tissue Res* 339: 237–246, 2010. doi:10.1007/s00441-009-0821-y.
- Iozzo RV, Schaefer L. Proteoglycan form and function: a comprehensive nomenclature of proteoglycans. *Matrix Biol* 42: 11–55, 2015. doi:10.1016/j.matbio.2015.02.003.
- Bülow HE, Hobert O. The molecular diversity of glycosaminoglycans shapes animal development. *Annu Rev Cell Dev Biol* 22: 375–407, 2006. doi:10.1146/annurev.cellbio.22.010605.093433.
- Sugahara K, Kitagawa H. Heparin and heparan sulfate biosynthesis. *IUBMB Life* 54: 163–175, 2002. doi:10.1080/15216540214928.
- Silbert JE, Sugumaran G. Biosynthesis of chondroitin/dermatan sulfate. *IUBMB Life* 54: 177–186, 2002. doi:10.1080/15216540290114450. doi:10.1080/15216540214923.
- Funderburgh JL. Keratan sulfate biosynthesis. *IUBMB Life* 54: 187–194, 2002. doi:10.1080/15216540290114469. doi:10.1080/15216540214932.
- Prydz K. Determinants of glycosaminoglycan (GAG) structure. *Biomolecules* 5: 2003–2022, 2015. doi:10.3390/biom5032003.
- Götting C, Kuhn J, Zahn R, Brinkmann T, Kleesiek K. Molecular cloning and expression of human UDP-D-xylose: proteoglycan core protein β -D-xylosyltransferase and its first isoform XT-II. *J Mol Biol* 304: 517–528, 2000. doi:10.1006/jmbi.2000.4261.
- Pönighaus C, Ambrosius M, Casanova JC, Prante C, Kuhn J, Esko JD, Kleesiek K, Götting C. Human xylosyltransferase II is involved in the biosynthesis of the uniform tetrasaccharide linkage region in chondroitin sulfate and heparan sulfate proteoglycans. *J Biol Chem* 282: 5201–5206, 2007. doi:10.1074/jbc.M611665200.
- Almeida R, Levery SB, Mandel U, Kresse H, Schwientek T, Bennett EP, Clausen H. Cloning and expression of a proteoglycan UDP-galactose: β -xylose β 1,4-galactosyltransferase I. A seventh member of the human β 4-galactosyltransferase gene family. *J Biol Chem* 274: 26165–26171, 1999. doi:10.1074/jbc.274.37.26165.
- Bai X, Zhou D, Brown JR, Crawford BE, Hennet T, Esko JD. Biosynthesis of the linkage region of glycosaminoglycans: cloning and activity of galactosyltransferase II, the sixth member of the β 1,3-galactosyltransferase family (beta 3GalT6). *J Biol Chem* 276: 48189–48195, 2001. doi:10.1074/jbc.M107339200.
- Kitagawa H, Tone Y, Tamura J, Neumann KW, Ogawa T, Oka S, Kawasaki T, Sugahara K. Molecular cloning and expression of glucuronyltransferase I involved in the biosynthesis of the glycosaminoglycan-protein linkage region of proteoglycans. *J Biol Chem* 273: 6615–6618, 1998. doi:10.1074/jbc.273.12.6615.
- Toledo AG, Nilsson J, Noborn F, Sihlbom C, Larson G. Positive mode LC-MS/MS analysis of chondroitin sulfate modified glycopeptides derived from light and heavy chains of the human inter- α -trypsin inhibitor complex. *Mol Cell Proteomics* 14: 3118–3131, 2015. doi:10.1074/mcp.M115.051136.
- Kitagawa H, Tsutsumi K, Ikegami-Kuzuhara A, Nadanaka S, Goto F, Ogawa T, Sugahara K. Sulfation of the galactose residues in the glycosaminoglycan-protein linkage region by recombinant human chondroitin 6-O-sulfotransferase-1. *J Biol Chem* 283: 27438–27443, 2008. doi:10.1074/jbc.M803279200.
- Sugahara K, Yamashina I, De Waard P, Van Halbeek H, Vliegthart JF. Structural studies on sulfated glycopeptides from the carbohydrate-protein linkage region of chondroitin 4-sulfate proteoglycans of swarm rat chondrosarcoma. Demonstration of the structure Gal(4-O-sulfate) β 1-3Gal β 1-4XYL β 1-O-Ser. *J Biol Chem* 263: 10168–10174, 1988. doi:10.1016/S0021-9258(19)81492-8.
- Koike T, Izumikawa T, Sato B, Kitagawa H. Identification of phosphatase that dephosphorylates xylose in the glycosaminoglycan-protein linkage region of proteoglycans. *J Biol Chem* 289: 6695–6708, 2014. doi:10.1074/jbc.M113.520536.
- Koike T, Izumikawa T, Tamura J-I, Kitagawa H. FAM20B is a kinase that phosphorylates xylose in the glycosaminoglycan-protein linkage region. *Biochem J* 421: 157–162, 2009. doi:10.1042/BJ20090474.
- McCormick C, Leduc Y, Martindale D, Mattison K, Esford L, Dyer A, Tufaro F. The putative tumour suppressor EXT1 alters the expression of cell-surface heparan sulfate. *Nat Genet* 19: 158–161, 1998. doi:10.1038/514.
- Lind T, Tufaro F, McCormick C, Lindahl U, Lidholt K. The putative tumor suppressors EXT1 and EXT2 are glycosyltransferases required for the biosynthesis of heparan sulfate. *J Biol Chem* 273: 26265–26268, 1998. doi:10.1074/jbc.273.41.26265.
- Kitagawa H, Shimakawa H, Sugahara K. The tumor suppressor EXT-like gene EXTL2 encodes an α 1,4-N-acetylhexosaminyltransferase that transfers N-acetylgalactosamine and N-acetylglucosamine to the common glycosaminoglycan-protein linkage region. The key enzyme for the chain initiation of heparin sulfate. *J Biol Chem* 274: 13933–13937, 1999. doi:10.1074/jbc.274.20.13933.
- Kim B-T, Kitagawa H, Tamura J, Saito T, Kusche-Gullberg M, Lindahl U, Sugahara K. Human tumor suppressor EXT gene family members EXTL1 and EXTL3 encode α 1,4-N-acetylglucosaminyltransferases that likely are involved in heparan sulfate/heparin biosynthesis. *Proc Natl Acad Sci USA* 98: 7176–7181, 2001. doi:10.1073/pnas.131188498.
- Busse M, Kusche-Gullberg M. In vitro polymerization of heparan sulfate backbone by the EXT proteins. *J Biol Chem* 278: 41333–41337, 2003. doi:10.1074/jbc.M308314200.
- Kim B-T, Kitagawa H, Tanaka J, Tamura J-I, Sugahara K. In vitro heparan sulfate polymerization: crucial roles of core protein moieties

- of primer substrates in addition to the EXT1-EXT2 interaction. *J Biol Chem* 278: 41618–41623, 2003. doi:10.1074/jbc.M304831200.
40. Kitagawa H, Uyama T, Sugahara K. Molecular cloning and expression of a human chondroitin synthase. *J Biol Chem* 276: 38721–38726, 2001. doi:10.1074/jbc.M106871200.
 41. Kitagawa H, Izumikawa T, Uyama T, Sugahara K. Molecular cloning of a chondroitin polymerizing factor that cooperates with chondroitin synthase for chondroitin polymerization. *J Biol Chem* 278: 23666–23671, 2003. doi:10.1074/jbc.M302493200.
 42. Uyama T, Kitagawa H, Tamura J-I, Sugahara K. Molecular cloning and expression of human chondroitin N-acetylgalactosaminyltransferase: the key enzyme for chain initiation and elongation of chondroitin/dermatan sulfate on the protein linkage region tetrasaccharide shared by heparin/heparan sulfate. *J Biol Chem* 277: 8841–8846, 2002. doi:10.1074/jbc.M111434200.
 43. Uyama T, Kitagawa H, Tanaka J, Tamura J-I, Ogawa T, Sugahara K. Molecular cloning and expression of a second chondroitin N-acetylgalactosaminyltransferase involved in the initiation and elongation of chondroitin/dermatan sulfate. *J Biol Chem* 278: 3072–3078, 2003. doi:10.1074/jbc.M209446200.
 44. Izumikawa T, Uyama T, Okuura Y, Sugahara K, Kitagawa H. Involvement of chondroitin sulfate synthase-3 (chondroitin synthase-2) in chondroitin polymerization through its interaction with chondroitin synthase-1 or chondroitin-polymerizing factor. *Biochem J* 403: 545–552, 2007. doi:10.1042/BJ20061876.
 45. Izumikawa T, Koike T, Shiozawa S, Sugahara K, Tamura J-I, Kitagawa H. Identification of chondroitin sulfate glucuronyltransferase as chondroitin synthase-3 involved in chondroitin polymerization: chondroitin polymerization is achieved by multiple enzyme complexes consisting of chondroitin synthase family members. *J Biol Chem* 283: 11396–11406, 2008. doi:10.1074/jbc.M707549200.
 46. Maccarana M, Olander B, Malmström J, Tiedemann K, Aebersold R, Lindahl U, Li J-P, Malmström A. Biosynthesis of dermatan sulfate: chondroitin-glucuronate C5-epimerase is identical to SART2. *J Biol Chem* 281: 11560–11568, 2006. doi:10.1074/jbc.M513373200.
 47. Pacheco B, Malmström A, Maccarana M. Two dermatan sulfate epimerases form iduronic acid domains in dermatan sulfate. *J Biol Chem* 284: 9788–9795, 2009. doi:10.1074/jbc.M809339200.
 48. Evers MR, Xia G, Kang HG, Schachner M, Baenziger JU. Molecular cloning and characterization of a dermatan-specific N-acetylgalactosamine 4-O-sulfotransferase. *J Biol Chem* 276: 36344–36353, 2001. doi:10.1074/jbc.M105848200.
 49. Mikami T, Mizumoto S, Kago N, Kitagawa H, Sugahara K. Specificities of three distinct human chondroitin/dermatan N-acetylgalactosamine 4-O-sulfotransferases demonstrated using partially desulfated dermatan sulfate as an acceptor: implication of differential roles in dermatan sulfate biosynthesis. *J Biol Chem* 278: 36115–36127, 2003. doi:10.1074/jbc.M306044200.
 50. Mizumoto S, Yamada S. Congenital disorders of deficiency in glycosaminoglycan biosynthesis. *Front Genet* 12: 717535, 2021. doi:10.3389/fgene.2021.717535.
 51. Malfait F, Castori M, Francomano CA, Giunta C, Kosho T, Byers PH. The Ehlers-Danlos syndromes. *Nat Rev Dis Primers* 6: 64, 2020. doi:10.1038/s41572-020-0194-9.
 52. Jansen LH. The structure of the connective tissue, an explanation of the symptoms of the Ehlers-Danlos syndrome. *Dermatologica* 110: 108–120, 1955. doi:10.1159/000256442.
 53. Beighton P, Paepe AD, Steinmann B, Tsipouras P, Wenstrup RJ. Ehlers-Danlos syndromes: revised nosology, Villefranche, 1997. Ehlers-Danlos National Foundation (USA) and Ehlers-Danlos Support Group (UK). *Am J Med Genet* 77: 31–37, 1998. doi:10.1002/(SICI)1096-8628(19980428)77:1<31::AID-AJMG8>3.0.CO;2-O.
 54. Malfait F, Francomano C, Byers P, Belmont J, Berglund B, Black J, et al. The 2017 international classification of the Ehlers-Danlos syndromes. *Am J Med Genet C Semin Med Genet* 175: 8–26, 2017. doi:10.1002/ajmg.c.31552.
 55. Hernández A, Aguirre-Negrete MG, Ramírez-Soltero S, González-Mendoza A, Martínez RM, Velázquez-Cabrera A, Cantú JM. A distinct variant of the Ehlers-Danlos syndrome. *Clin Genet* 16: 335–339, 1979. doi:10.1111/j.1399-0004.1979.tb01012.x.
 56. Hernández A, Aguirre-Negrete MG, González-Flores S, Reynoso-Luna MC, Fragoso R, Nazaré Z, Tapia-Arizmendi G, Cantú JM. Ehlers-Danlos features with progeroid facies and mild mental retardation. Further delineation of the syndrome. *Clin Genet* 30: 456–461, 1986. doi:10.1111/j.1399-0004.1986.tb01910.x.
 57. Hernández A, Aguirre-Negrete MG, Liparoli JC, Cantú JM. Third case of a distinct variant of the Ehlers-Danlos Syndrome (EDS). *Clin Genet* 20: 222–224, 1981. doi:10.1111/j.1399-0004.1981.tb01833.x.
 58. Kresse H, Rosthøj S, Quentin E, Hollmann J, Glössl J, Okada S, Tønnesen T. Glycosaminoglycan-free small proteoglycan core protein is secreted by fibroblasts from a patient with a syndrome resembling progeroid. *Am J Hum Genet* 41: 436–453, 1987.
 59. Quentin E, Gladen A, Rodén L, Kresse H. A genetic defect in the biosynthesis of dermatan sulfate proteoglycan: galactosyltransferase I deficiency in fibroblasts from a patient with a progeroid syndrome. *Proc Natl Acad Sci USA* 87: 1342–1346, 1990. doi:10.1073/pnas.87.4.1342.
 60. Okajima T, Fukumoto S, Furukawa K, Urano T, Furukawa K. Molecular basis for the progeroid variant of Ehlers-Danlos Syndrome. Identification and characterization of two mutations in galactosyltransferase I gene. *J Biol Chem* 274: 28841–28844, 1999. doi:10.1074/jbc.274.41.28841.
 61. Danielson KG, Baribault H, Holmes DF, Graham H, Kadler KE, Iozzo RV. Targeted disruption of decorin leads to abnormal collagen fibril morphology and skin fragility. *J Cell Biol* 136: 729–743, 1997. doi:10.1083/jcb.136.3.729.
 62. Corsi A, Xu T, Chen X-D, Boyde A, Liang J, Mankani M, Sommer B, Iozzo RV, Eichstetter I, Robey PG, Bianco P, Young MF. Phenotypic effects of biglycan deficiency are linked to collagen fibril abnormalities, are synergized by decorin deficiency, and mimic Ehlers-Danlos-like changes in bone and other connective tissues. *J Bone Miner Res* 17: 1180–1189, 2002. doi:10.1359/jbmr.2002.17.7.1180.
 63. Heegaard A-M, Corsi A, Danielsen CC, Nielsen KL, Jorgensen HL, Riminucci M, Young MF, Bianco P. Biglycan deficiency causes spontaneous aortic dissection and rupture in mice. *Circulation* 115: 2731–2738, 2007. doi:10.1161/CIRCULATIONAHA.106.653980.
 64. Chakravarti S, Petroll WM, Hassell JR, Jester JV, Lass JH, Paul J, Birk DE. Corneal opacity in lumican-null mice: defects in collagen fibril structure and packing in the posterior stroma. *Invest Ophthalmol Vis Sci* 41: 3365–3373, 2000.
 65. Svensson L, Aszodi A, Reinholt FP, Fässler R, Heinegård D, Oldberg Å. Fibromodulin-null mice have abnormal collagen fibrils, tissue organization, and altered lumican deposition in tendon. *J Biol Chem* 274: 9636–9647, 1999. doi:10.1074/jbc.274.14.9636.
 66. Ezura Y, Chakravarti S, Oldberg Å, Chervoneva I, Birk DE. Differential expression of lumican and fibromodulin regulate collagen fibrillogenesis in developing mouse tendons. *J Cell Biol* 151: 779–788, 2000. doi:10.1083/jcb.151.4.779.
 67. Jepsen KJ, Wu F, Peragallo JH, Paul J, Roberts L, Ezura Y, Oldberg Å, Birk DE, Chakravarti S. A syndrome of joint laxity and impaired tendon integrity in lumican- and fibromodulin-deficient mice. *J Biol Chem* 277: 35532–35540, 2002. doi:10.1074/jbc.M205398200.
 68. Ameye L, Aria D, Jepsen K, Oldberg Å, Xu T, Young MF. Abnormal collagen fibrils in tendons of biglycan/fibromodulin-deficient mice lead to gait impairment, ectopic ossification, and osteoarthritis. *FASEB J* 16: 673–680, 2002. doi:10.1096/fj.01-0848com.
 69. Ameye L, Young MF. Mice deficient in small leucine-rich proteoglycans: novel in vivo models for osteoporosis, osteoarthritis, Ehlers-Danlos syndrome, muscular dystrophy, and connective diseases. *Glycobiology* 12: 107R–116R, 2002. doi:10.1093/glycob/cwf065.
 70. Malfait F, Coucke P, Symoens S, Loeys B, Nuytinck L, De Paepe A. The molecular basis of classic Ehlers-Danlos syndrome: a comprehensive study of biochemical and molecular findings in 48 unrelated patients. *Hum Mutat* 25: 28–37, 2005. doi:10.1002/humu.20107.
 71. Dündar M, Müller T, Zhang Q, Pan J, Steinmann B, Vodopitiz J, Gruber R, Sonoda T, Krabichler B, Utermann G, Baenziger JU, Zhang L, Jancke AR. Loss of dermatan-4-sulfotransferase 1 function results in adducted thumb-clubfoot syndrome. *Am J Hum Genet* 85: 873–882, 2009. doi:10.1016/j.ajhg.2009.11.010.
 72. Miyake N, Kosho T, Mizumoto S, Furuichi T, Hatamochi A, Nagashima Y, Arai E, Takahashi K, Kawamura R, Wakui K, Takahashi J, Kato H, Yasui H, Ishida T, Ohashi H, Nishimura G, Shiina M, Saito H, Tsurusaki Y, Doi H, Fukushima Y, Ikegawa S, Yamada S, Sugahara K, Matsumoto N. Loss-of-function mutations of CHST14 in a new type of Ehlers-Danlos syndrome. *Hum Mutat* 31: 966–974, 2010. doi:10.1002/humu.21300.
 73. Kosho T, Miyake N, Hatamochi A, Takahashi J, Kato H, Miyahara T, Igawa Y, Yasui H, Ishida T, Ono K, Kosuda T, Inoue A, Kohyama M,

- Hattori T, Ohashi H, Nishimura G, Kawamura R, Wakui K, Fukushima Y, Matsumoto N. A new Ehlers-Danlos syndrome with craniofacial characteristics, multiple congenital contractures, progressive joint and skin laxity, and multisystem fragility-related manifestations. *Am J Med Genet Part A* 152A: 1333–1346, 2010. doi:10.1002/ajmg.a.33498.
74. Malfait F, Syx D, Vliummens P, Symoens S, Nampoothiri S, Hermanns-Lê T, Van Laer L, De Paepe A. Musculocontractural Ehlers-Danlos Syndrome (former EDS type VIB) and adducted thumb clubfoot syndrome (ATCS) represent a single clinical entity caused by mutations in the dermatan-4-sulfotransferase 1 encoding CHST14 gene. *Hum Mutat* 31: 1233–1239, 2010. doi:10.1002/humu.21355.
75. Müller T, Mizumoto S, Suresh I, Komatsu Y, Vodopietz J, Dunder M, Straub V, Lingenhel A, Melmer A, Lechner S, Zschocke J, Sugahara K, Janeczek AR. Loss of dermatan sulfate epimerase (DSE) function results in musculocontractural Ehlers-Danlos syndrome. *Hum Mol Genet* 22: 3761–3772, 2013. doi:10.1093/hmg/ddt227.
76. Syx D, Van Damme T, Symoens S, Maiburg MC, van de Laar I, Morton J, Suri M, Del Campo M, Hausser I, Hermanns-Lê T, De Paepe A, Malfait F. Genetic heterogeneity and clinical variability in musculocontractural ehlers-danlos syndrome caused by impaired dermatan sulfate biosynthesis. *Hum Mutat* 36: 535–547, 2015. doi:10.1002/humu.22774.
77. Malfait F, Kariminejad A, Van Damme T, Gauche C, Syx D, Merhi-Soussi F, Gulberti S, Symoens S, Vanhauwaert S, Willaert A, Bozorgmehr B, Kariminejad MH, Ebrahimiadib N, Hausser I, Huyseune A, Fournel-Gigleux S, De Paepe A. Defective initiation of glycosaminoglycan synthesis due to B3GALT6 mutations causes a pleiotropic Ehlers-Danlos-syndrome-like connective tissue disorder. *Am J Hum Genet* 92: 935–945, 2013. doi:10.1016/j.ajhg.2013.04.016.
78. Nakajima M, Mizumoto S, Miyake N, Kogawa R, Iida A, Ito H, Kitoh H, Hirayama A, Mitsubuchi H, Miyazaki O, Kosaki R, Horikawa R, Lai A, Mendoza-Londono R, Dupuis L, Chitayat D, Howard A, Leal GF, Cavalcanti D, Tsurusaki Y, Saitsu H, Watanabe S, Lausch E, Unger S, Bonafé L, Ohashi H, Superti-Furga A, Matsumoto N, Sugahara K, Nishimura G, Ikegawa S. Mutations in B3GALT6, which encodes a glycosaminoglycan linker region enzyme, cause a spectrum of skeletal and connective tissue disorders. *Am J Hum Genet* 92: 927–934, 2013. doi:10.1016/j.ajhg.2013.04.003.
79. Sandler-Wilson C, Wambach JA, Marshall BA, Wegner DJ, McAlister W, Cole FS, Shinawi M. Phenotype and response to growth hormone therapy in siblings with B4GALT7 deficiency. *Bone* 124: 14–21, 2019. doi:10.1016/j.bone.2019.03.029.
80. Mihalic Mosher T, Zygmunt DA, Koboldt DC, Kelly BJ, Johnson LR, McKenna DS, Hood BC, Hickey SE, White P, Wilson RK, Martin PT, McBride KL. Expansion of B4GALT7 linkeropathy phenotype to include perinatal lethal skeletal dysplasia. *Eur J Hum Genet* 27: 1569–1577, 2019. doi:10.1038/s41431-019-0464-8.
81. Caraffi SG, Maini I, Ivanovski I, Pollazzon M, Giangioffe S, Valli M, Rossi A, Sassi S, Faccioli S, Rocco MD, Magnani C, Campos-Xavier B, Unger S, Superti-Furga A, Garavelli L. Severe peripheral joint laxity is a distinctive clinical feature of spondylodysplastic-ehlersdanlos syndrome (Eds)-B4GALT7 and spondylodysplastic-EDS-b3GALT6. *Genes (Basel)* 10: 799, 2019. doi:10.3390/genes10100799.
82. Wang J, Wang Y, Wang L, Chen WY, Sheng M. The diagnostic yield of intellectual disability: combined whole genome low-coverage sequencing and medical exome sequencing. *BMC Med Genomics* 13: 70, 2020. doi:10.1186/s12920-020-0726-x.
83. Lorenz D, Kress W, Zaum A-K, Speer CP, Hebestreit H. Report of two siblings with spondylodysplastic Ehlers-Danlos syndrome and B4GALT7 deficiency. *BMC Pediatr* 21: 293, 2021. doi:10.1186/s12887-021-02767-0.
84. Faiyaz-UI-Haque M, Zaidi SHE, Al-Ali M, Al-Mureikhi MS, Kennedy S, Al-Thani G, Tsui L-C, Teebi AS. A novel missense mutation in the galactosyltransferase-I (B4GALT7) gene in a family exhibiting facioskeletal anomalies and Ehlers-Danlos syndrome resembling the progeroid type. *Am J Med Genet* 128 A: 39–45, 2004. doi:10.1002/ajmg.a.30005.
85. Guo MH, Shen Y, Walvoord EC, Miller TC, Moon JE, Hirschhorn JN, Dauber A. Whole exome sequencing to identify genetic causes of short stature. *Horm Res Paediatr* 82: 44–52, 2014. doi:10.1159/000360857.
86. Cartault F, Munier P, Jacquemont ML, Vellayoudom J, Doray B, Payet C, Randrianaivo H, Laville JM, Munnich A, Cormier-Daire V. Expanding the clinical spectrum of B4GALT7 deficiency: Homozygous p.R270C mutation with founder effect causes Larsen of Reunion Island syndrome. *Eur J Hum Genet* 23: 49–53, 2015. doi:10.1038/ejhg.2014.60.
87. Deciphering Developmental Disorders Study. Large-scale discovery of novel genetic causes of developmental disorders. *Nature* 519: 223–228, 2015. doi:10.1038/nature14135.
88. Salter CG, Davies JH, Moon RJ, Fairhurst J, Bunyan D; DDD Study; Foulds N. Further defining the phenotypic spectrum of B4GALT7 mutations. *Am J Med Genet A* 170: 1556–1563, 2016. doi:10.1002/ajmg.a.37604.
89. Arunrut T, Sabbadini M, Jain M, Machol K, Scaglia F, Slavotinek A. Corneal clouding, cataract, and colobomas with a novel missense mutation in B4GALT7—a review of eye anomalies in the linkeropathy syndromes. *Am J Med Genet A* 170: 2711–2718, 2016. doi:10.1002/ajmg.a.37809.
90. Ranza E, Huber C, Levin N, Baujat G, Bole-Feysot C, Nitschke P, Masson C, Alanay Y, Al-Gazali L, Bitoun P, Boute O, Campeau P, Coubes C, McEntagart M, Elcioglu N, Faivre L, Gezdirici A, Johnson D, Mihci E, Nur BG, Perrin L, Quelin C, Terhal P, Tuysuz B, Cormier-Daire V. Chondrodysplasia with multiple dislocations: comprehensive study of a series of 30 cases. *Clin Genet* 91: 868–880, 2017. doi:10.1111/cge.12885.
91. Ritelli M, Dordoni C, Cinquina V, Venturini M, Calzavara-Pinton P, Colombi M. Expanding the clinical and mutational spectrum of B4GALT7-spondylodysplastic Ehlers-Danlos syndrome. *Orphanet J Rare Dis* 12: 153, 2017. doi:10.1186/s13023-017-0704-3.
92. Trejo P, Rauch F, Glorieux FH, Ouellet J, Benaroch T, Campeau PM. Spondyloepimetaphyseal dysplasia with joint laxity in three siblings with B3GALT6 mutations. *Mol Syndromol* 8: 303–307, 2017. doi:10.1159/000479672.
93. Ben-Mahmoud A, Ben-Salem S, Al-Sorkhy M, John A, Ali BR, Al-Gazali L. A B3GALT6 variant in patient originally described as Al-Gazali syndrome and implicating the endoplasmic reticulum quality control in the mechanism of some β 3GalT6-pathway mutations. *Clin Genet* 93: 1148–1158, 2018. doi:10.1111/cge.13236.
94. Maddirevula S, Alsahli S, Alhabeib L, Patel N, Alzahrani F, Shamseldin HE, et al. Expanding the phenome and variome of skeletal dysplasia. *Genet Med* 20: 1609–1616, 2018. doi:10.1038/gim.2018.50.
95. Van Damme T, Pang X, Guillemin B, Gulberti S, Syx D, De Rycke R, Kaye O, de Die-Smulders CEM, Pfundt R, Kariminejad A, Nampoothiri S, Pierquin G, Bulk S, Larson AA, Chatfield KC, Simon M, Legrand A, Gerard M, Symoens S, Fournel-Gigleux S, Malfait F. Biallelic B3GALT6 mutations cause spondylodysplastic Ehlers-Danlos syndrome. *Hum Mol Genet* 27: 3475–3487, 2018. doi:10.1093/hmg/ddy234.
96. Leoni C, Tedesco M, Radio FC, Chillemi G, Leone A, Bruxelles A, Cioffi A, Stellacci E, Pantaleoni F, Butera G, Rigante D, Onesimo R, Tartaglia M, Zampino G. Broadening the phenotypic spectrum of Beta3GalT6-associated phenotypes. *Am J Med Genet A* 185: 3153–3160, 2021. doi:10.1002/ajmg.a.62399.
97. Descartes M, Melenevsky YV, Rudy N, Smith K, Callaway K, Parker JS. Keratoconus in a patient with B3GALT6-related disorder. *Clin Genet* 99: 849–850, 2021. doi:10.1111/cge.13940.
98. Silveira KC, Kanazawa TY, Silveira C, Lacarrubba-Flores MDJ, Carvalho BS, Cavalcanti DP. Molecular diagnosis in a cohort of 114 patients with rare skeletal dysplasias. *Am J Med Genet C Semin Med Genet* 187: 396–408, 2021. doi:10.1002/ajmg.c.31937.
99. Zhang J, Huang K, Dong G. Clinical and genetic analysis of a child with spondyloepimetaphyseal dysplasia type 1 and joint laxity. *Zhonghua Yi Xue Yi Chuan Xue Za Zhi* 37: 887–890, 2020. doi:10.3760/cma.j.issn.1003-9406.2020.08.020.
100. Vorster AA, Beighton P, Ramesar RS. Spondyloepimetaphyseal dysplasia with joint laxity (Beighton type); mutation analysis in eight affected South African families. *Clin Genet* 87: 492–495, 2015. doi:10.1111/cge.12413.
101. Sellars EA, Bosanko KA, Lepard T, Garnica A, Schaefer GB. A newborn with complex skeletal abnormalities, joint contractures, and bilateral corneal clouding with sclerocornea. *Semin Pediatr Neurol* 21: 84–87, 2014. doi:10.1016/j.spen.2014.04.007.
102. Ritelli M, Chiarelli N, Zoppi N, Dordoni C, Quinzani S, Traversa M, Venturini M, Calzavara-Pinton P, Colombi M. Insights in the etiopathology of galactosyltransferase II (GalT-II) deficiency from

- transcriptome-wide expression profiling of skin fibroblasts of two sisters with compound heterozygosity for two novel B3GALT6 mutations. *Mol Genet Metab Rep* 2: 1–15, 2015. doi:10.1016/j.ymgmr.2014.11.005.
103. Alazami AM, Al-Qattan SM, Faqeih E, Alhashem A, Alshammari M, Alzahrani F, Al-Dosari MS, Patel N, Alsagheir A, Binabbas B, Alzaidan H, Alsiddiky A, Alharbi N, Alfadhel M, Kentab A, Daza RM, Kircher M, Shendure J, Hashem M, Alshahrani S, Rahbeeni Z, Khalifa O, Shaheen R, Alkuraya FS. Expanding the clinical and genetic heterogeneity of hereditary disorders of connective tissue. *Hum Genet* 135: 525–540, 2016. doi:10.1007/s00439-016-1660-z.
 104. Honey EM. Spondyloepimetaphyseal dysplasia with joint laxity (Beighton type): a unique South African disorder. *S Afr Med J* 106: S54–S56, 2016. doi:10.7196/SAMJ.2016.v106i6.10994.
 105. Brockel M, Chatfield K, Mirsky D, Baker CD, Janosy N. Anesthetic considerations for a child with rare B3GALT6 mutations: a case report. *A A Pract* 10: 83–86, 2018. doi:10.1213/xxa.0000000000000638.
 106. Janecke AR, Li B, Boehm M, Krabichler B, Rohrbach M, Müller T, Fuchs I, Golas G, Katagiri Y, Ziegler SG, Gahl WA, Wilnai Y, Zoppi N, Geller HM, Giunta C, Slavotinek A, Steinmann B. The phenotype of the musculocontractural type of Ehlers-Danlos syndrome due to CHST14 mutations. *Am J Med Genet Part A* 170A: 103–115, 2016. doi:10.1002/ajmg.a.37383.
 107. Minatogawa M, Unzaki A, Morisaki H, Syx D, Sonoda T, Janecke AR, et al. Clinical and molecular features of 66 patients with musculocontractural Ehlers–Danlos syndrome caused by pathogenic variants in *CHST14* (mcEDS- *CHST14*). *J Med Genet* 59: 865–877, 2022. doi:10.1136/jmedgenet-2020-107623.
 108. Uehara M, Kosho T, Yamamoto N, Takahashi HE, Shimakura T, Nakayama J, Kato H, Takahashi J. Spinal manifestations in 12 patients with musculocontractural Ehlers-Danlos syndrome caused by *CHST14*/*D4ST1* deficiency (mcEDS-*CHST14*). *Am J Med Genet A* 176: 2331–2341, 2018. doi:10.1002/ajmg.a.40507.
 109. Kono M, Hasegawa-Murakami Y, Sugiura K, Ono M, Toriyama K, Miyake N, Hatamochi A, Kamei Y, Kosho T, Akiyama M. A 45-year-old woman with Ehlers-Danlos syndrome caused by dermatan 4-O-sulfotransferase-1 deficiency: implications for early ageing. *Acta Derm Venereol* 96: 830–831, 2016. doi:10.2340/00015555-2390.
 110. Mochida K, Amano M, Miyake N, Matsumoto N, Hatamochi A, Kosho T. Dermatan 4-O-sulfotransferase 1-deficient Ehlers-Danlos syndrome complicated by a large subcutaneous hematoma on the back. *J Dermatol* 43: 832–833, 2016. doi:10.1111/1346-8138.13273.
 111. Uehara M, Oba H, Hatakenaka T, Ikegami S, Kuraishi S, Takizawa T, Munakata R, Mimura T, Yamaguchi T, Kosho T, Takahashi J. Posterior spinal fusion for severe spinal deformities in musculocontractural Ehlers-Danlos syndrome: detailed observation of a novel case and review of 2 reported cases. *World Neurosurg* 143: 454–461, 2020. doi:10.1016/j.wneu.2020.08.085.
 112. Sandal S, Kaur A, Panigrahi I. Novel mutation in the *CHST14* gene causing musculocontractural type of Ehlers-Danlos syndrome. *BMJ Case Rep* 2018: bcr-2018-226165, 2018. doi:10.1136/bcr-2018-226165.
 113. Anazi S, Maddirevula S, Faqeih E, Alsedairy H, Alzahrani F, Shamseldin HE, et al. Clinical genomics expands the morbid genome of intellectual disability and offers a high diagnostic yield. *Mol Psychiatry* 22: 615–624, 2017. doi:10.1038/mp.2016.113.
 114. Shimizu K, Okamoto N, Miyake N, Taira K, Sato Y, Matsuda K, Akimaru N, Ohashi H, Wakui K, Fukushima Y, Matsumoto N, Kosho T. Delineation of dermatan 4-O-sulfotransferase 1 deficient Ehlers-Danlos syndrome: Observation of two additional patients and comprehensive review of 20 reported patients. *Am J Med Genet Part A* 155A: 1949–1958, 2011. doi:10.1002/ajmg.a.34115.
 115. Voermans NC, Kempers M, Lammens M, Van Alfen N, Janssen MC, Bönnemann C, Van Engelen BG, Hamel BC. Myopathy in a 20-year-old female patient with *D4ST1* deficient Ehlers-Danlos syndrome due to a homozygous *CHST14* mutation. *Am J Med Genet Part A* 158A: 850–855, 2012. doi:10.1002/ajmg.a.35232.
 116. Mendoza-Londono R, Chitayat D, Kahr WHA, Hinek A, Blaser S, Dupuis L, Goh E, Badilla-Porras R, Howard A, Mittaz L, Superti-Furga A, Unger S, Nishimura G, Bonafe L. Extracellular matrix and platelet function in patients with musculocontractural Ehlers-Danlos syndrome caused by mutations in the *CHST14* gene. *Am J Med Genet Part A* 158A: 1344–1354, 2012. doi:10.1002/ajmg.a.35339.
 117. Winters KA, Jiang Z, Xu W, Li S, Ammous Z, Jayakar P, Wierenga KJ. Re-assigned diagnosis of *D4ST1*-deficient Ehlers-Danlos syndrome (adducted thumb-clubfoot syndrome) after initial diagnosis of Marden-Walker syndrome. *Am J Med Genet Part A* 158A: 2935–2940, 2012. doi:10.1002/ajmg.a.35613.
 118. Lautrup CK, Teik KW, Unzaki A, Mizumoto S, Syx D, Sin HH, Nielsen IK, Markholt S, Yamada S, Malfait F, Matsumoto N, Miyake N, Kosho T. Delineation of musculocontractural Ehlers–Danlos Syndrome caused by dermatan sulfate epimerase deficiency. *Mol Genet Genomic Med* 8: e1197, 2020. doi:10.1002/mgg3.1197.
 119. Schirwani S, Metcalfe K, Wagner B, Berry I, Sobey G, Jewell R. DSE associated musculocontractural EDS, a milder phenotype or phenotypic variability. *Eur J Med Genet* 63: 103798, 2020. doi:10.1016/j.ejmg.2019.103798.
 120. Ullah I, Aamir M, Ilyas M, Ahmed A, Jelani M, Ullah W, Abbas M, Ishfaq M, Ali F, Yip J, Efthymiou S, Ahmed H, Houlden H. A novel variant in the *DSE* gene leads to Ehlers–Danlos musculocontractural type 2 in a Pakistani family. *Congenit Anom (Kyoto)* 61: 177–182, 2021. doi:10.1111/cga.12436.
 121. Vroman R, Malfait A-M, Miller RE, Malfait F, Syx D. Animal models of Ehlers–Danlos syndromes: phenotype, pathogenesis, and translational potential. *Front Genet* 12: 726474, 2021. doi:10.3389/fgene.2021.726474.
 122. Seidler DG, Faiyaz-UI-Haque M, Hansen U, Yip GW, Zaidi SHE, Teebi AS, Kiesel L, Götte M. Defective glycosylation of decorin and biglycan, altered collagen structure, and abnormal phenotype of the skin fibroblasts of an Ehlers-Danlos syndrome patient carrying the novel Arg270Cys substitution in galactosyltransferase I (β 4GalT-7). *J Mol Med (Berl)* 84: 583–594, 2006. doi:10.1007/s00109-006-0046-4.
 123. Götte M, Spillmann D, Yip GW, Versteeg E, Echtermeyer FG, Van Kuppevelt TH, Kiesel L. Changes in heparan sulfate are associated with delayed wound repair, altered cell migration, adhesion and contractility in the galactosyltransferase I (β 4GalT-7) deficient form of Ehlers-Danlos syndrome. *Hum Mol Genet* 17: 996–1009, 2008. doi:10.1093/hmg/ddm372.
 124. Haouari W, Dubail J, Lounis-Ouaras S, Prada P, Bennani R, Roseau C, Huber C, Afejar A, Colin E, Vuillaumier-Barrot S, Seta N, Foulquier F, Poüs C, Cormier-Daire V, Bruneel A. Serum bikunin isoforms in congenital disorders of glycosylation and linkeropathies. *J Inher Metab Dis* 43: 1349–1359, 2020. doi:10.1002/jimd.12291.
 125. Bruneel A, Dubail J, Roseau C, Prada P, Haouari W, Huber C, Dupré T, Poüs C, Cormier-Daire V, Seta N. Serum bikunin is a biomarker of linkeropathies. *Clin Chim Acta* 485: 178–180, 2018. doi:10.1016/j.cca.2018.06.044.
 126. Bui C, Talhaoui I, Chabel M, Mulliert G, Coughtrie MWH, Ouzzine M, Fournel-Gigleux S. Molecular characterization of β 1,4-galactosyltransferase 7 genetic mutations linked to the progeroid form of Ehlers-Danlos syndrome (EDS). *FEBS Lett* 584: 3962–3968, 2010. doi:10.1016/j.febslet.2010.08.001.
 127. Guo MH, Stoler J, Lui J, Nilsson O, Bianchi DW, Hirschhorn JN, Dauber A. Redefining the progeroid form of ehlers-danlos syndrome: Report of the fourth patient with *B4GALT7* deficiency and review of the literature. *Am J Med Genet Part A* 161A: 2519–2527, 2013. doi:10.1002/ajmg.a.36128.
 128. Delbaere S, Van Damme T, Syx D, Symoens S, Coucke P, Willaert A, Malfait F. Hypomorphic zebrafish models mimic the musculoskeletal phenotype of β 4GalT7-deficient Ehlers-Danlos syndrome. *Matrix Biol* 89: 59–75, 2020. doi:10.1016/j.matbio.2019.12.002.
 129. Leegwater PA, Vos-Loohuis M, Ducro BJ, Boegheim IJ, Steenbeek FG, Nijman IJ, Monroe GR, Bastiaansen JWM, Dibbitts BW, Goor LH, Hellinga I, Back W, Schurink A. Dwarfism with joint laxity in Friesian horses is associated with a splice site mutation in *B4GALT7*. *BMC Genomics* 17: 839, 2016. doi:10.1186/s12864-016-3186-0.
 130. Delbaere S, De Clercq A, Mizumoto S, Noborn F, Bek JW, Alluyn L, Gistelincx C, Syx D, Salmon PL, Coucke PJ, Larson G, Yamada S, Willaert A, Malfait F. *b3galt6* knock-out zebrafish recapitulate β 3GalT6-deficiency disorders in human and reveal a trisaccharide proteoglycan linkage region. *Front Cell Dev Biol* 8: 597857, 2020. doi:10.3389/fcell.2020.597857.
 131. Persson A, Nilsson J, Vorontsov E, Noborn F, Larson G. Identification of a non-canonical chondroitin sulfate linkage region trisaccharide. *Glycobiology* 29: 366–371, 2019. doi:10.1093/glycob/cvz014.
 132. Nikpour M, Noborn F, Nilsson J, Van Damme T, Kaye O, Syx D, Malfait F, Larson G. Glycosaminoglycan linkage region of urinary

- bikunin as a potentially useful biomarker for β 3GalT6-deficient spondylo dysplastic Ehlers–Danlos syndrome. *JIMD Reports* 29: 366–371, 2022. doi:10.1002/jmd2.12311.
133. Mizumoto S, Kosho T, Hatamochi A, Honda T, Yamaguchi T, Okamoto N, Miyake N, Yamada S, Sugahara K. Defect in dermatan sulfate in urine of patients with Ehlers–Danlos syndrome caused by a CHST14/D4ST1 deficiency. *Clin Biochem* 50: 670–677, 2017. doi:10.1016/j.clinbiochem.2017.02.018.
134. Malmström A. Biosynthesis of dermatan sulfate. II. Substrate specificity of the C-5 uronosyl epimerase. *J Biol Chem* 259: 161–165, 1984. doi:10.1016/S0021-9258(17)43635-0.
135. Nomura Y. Structural change in decorin with skin aging. *Connect Tissue Res* 47: 249–255, 2006. doi:10.1080/03008200600846606.
136. Hirose T, Takahashi N, Tangkawattana P, Minaguchi J, Mizumoto S, Yamada S, Miyake N, Hayashi S, Hatamochi A, Nakayama J, Yamaguchi T, Hashimoto A, Nomura Y, Takehana K, Kosho T, Watanabe T. Structural alteration of glycosaminoglycan side chains and spatial disorganization of collagen networks in the skin of patients with mcEDS-CHST14. *Biochim Biophys Acta Gen Subj* 1863: 623–631, 2019. doi:10.1016/j.bbagen.2018.12.006.
137. Yoshizawa T, Mizumoto S, Takahashi Y, Shimada S, Sugahara K, Nakayama J, Takeda S, Nomura Y, Nitahara-Kasahara Y, Okada T, Matsumoto K, Yamada S, Kosho T. Vascular abnormalities in the placenta of Chst14-/- fetuses: implications in the pathophysiology of perinatal lethality of the murine model and vascular lesions in human CHST14/D4ST1 deficiency. *Glycobiology* 28: 80–89, 2018. doi:10.1093/glycob/cwx099.
138. Akyüz N, Rost S, Mehanna A, Bian S, Loers G, Oezen I, Mishra B, Hoffmann K, Guseva D, Laczynska E, Irintchev A, Jakovcevski I, Schachner M. Dermatan 4-O-sulfotransferase1 ablation accelerates peripheral nerve regeneration. *Exp Neurol* 247: 517–530, 2013. doi:10.1016/j.expneurol.2013.01.025.
139. Nitahara-Kasahara Y, Mizumoto S, Inoue YU, Saka S, Posadas-Herrera G, Nakamura-Takahashi A, Takahashi Y, Hashimoto A, Konishi K, Miyata S, Masuda C, Matsumoto E, Maruoka Y, Yoshizawa T, Tanase T, Inoue T, Yamada S, Nomura Y, Takeda S, Watanabe A, Kosho T, Okada T. A new mouse model of Ehlers–Danlos syndrome generated using CRISPR/Cas9-mediated genomic editing. *Dis Model Mech* 14: dmm048963, 2021. doi:10.1242/dmm.048963.
140. Hirose T, Mizumoto S, Hashimoto A, Takahashi Y, Yoshizawa T, Nitahara-Kasahara Y, Takahashi N, Nakayama J, Takehana K, Okada T, Nomura Y, Yamada S, Kosho T, Watanabe T. Systematic investigation of the skin in Chst14-/- mice: a model for skin fragility in musculocontractural Ehlers–Danlos syndrome caused by CHST14 variants (mcEDS-CHST14). *Glycobiology* 31: 137–150, 2021. doi:10.1093/glycob/cwaa058.
141. Nitahara-Kasahara Y, Posadas-Herrera G, Mizumoto S, Nakamura-Takahashi A, Inoue YU, Inoue T, Nomura Y, Takeda S, Yamada S, Kosho T, Okada T. Myopathy associated with dermatan sulfate-deficient decorin and myostatin in musculocontractural Ehlers–Danlos syndrome: a mouse model investigation. *Front Cell Dev Biol* 9: 695021, 2021. doi:10.3389/fcell.2021.695021.
142. Rost S, Akyüz N, Martinovic T, Huckhagel T, Jakovcevski I, Schachner M. Germline ablation of dermatan-4O-sulfotransferase1 reduces regeneration after mouse spinal cord injury. *Neuroscience* 312: 74–85, 2016. doi:10.1016/j.neuroscience.2015.11.013.
143. Li Q, Wu X, Na X, Ge B, Wu Q, Guo X, Ntim M, Zhang Y, Sun Y, Yang J, Xiao Z, Zhao J, Li S. Impaired cognitive function and altered hippocampal synaptic plasticity in mice lacking dermatan sulfotransferase Chst14/D4st1. *Front Mol Neurosci* 12: 26, 2019. doi:10.3389/fnmol.2019.00026.
144. Maccarana M, Kalamajski S, Kongsgaard M, Magnusson SP, Oldberg Å, Malmström A. Dermatan sulfate epimerase 1-deficient mice have reduced content and changed distribution of iduronic acids in dermatan sulfate and an altered collagen structure in skin. *Mol Cell Biol* 29: 5517–5528, 2009. doi:10.1128/mcb.00430-09.
145. Gustafsson R, Stachtea X, Maccarana M, Grottlings E, Eklund E, Malmström A, Oldberg Å. Dermatan sulfate epimerase 1 deficient mice as a model for human abdominal wall defects. *Birth Defects Res A Clin Mol Teratol* 100: 712–720, 2014. doi:10.1002/bdra.23300.
146. Stachtea XN, Tykesson E, van Kuppevelt TH, Feinstein R, Malmström A, Reijmers RM, Maccarana M. Dermatan sulfate-free mice display embryological defects and are neonatal lethal despite normal lymphoid and non-lymphoid organogenesis. *PLoS One* 10: e0140279, 2015. doi:10.1371/journal.pone.0140279.
147. Haouari W, Dubail J, Poüs C, Cormier-Daire V, Bruneel A. Inherited proteoglycan biosynthesis defects—current laboratory tools and bikunin as a promising blood biomarker. *Genes (Basel)* 12: 1654, 2021. doi:10.3390/genes1211654.